NAVAL POSTGRADUATE SCHOOL

MONTEREY, CALIFORNIA

THESIS

SHIPBOARD RADIO FREQUENCY AND FREE SPACE OPTICS COMMUNICATIONS SYSTEM USING AN AIRBORNE RELAY

by

Kenneth St. Germain

September 2005

Thesis Advisor:	Frank Kragh
Second Reader:	Tri Ha

Approved for public release; distribution is unlimited.

THIS PAGE INTENTIONALLY LEFT BLANK

REPORT DOCUMENTATION PAGE			Form Approved OMB No. 0704-0188
Public reporting burden for this collection of information is estimated to average 1 hour per response, including the time for reviewing instruction, searching existing data sources, gathering and maintaining the data needed, and completing and reviewing the collection of information. Send comments regarding this burden estimate or any other aspect of this collection of information, including suggestions for reducing this burden, to Washington headquarters Services, Directorate for Information Operations and Reports, 1215 Jefferson Davis Highway, Suite 1204, Arlington, VA 22202-4302, and to the Office of Management and Budget, Paperwork Reduction Project (0704-0188) Washington DC 20503.			
1. AGENCY USE ONLY ***(Leave blank)***	**2. REPORT DATE** September 2005	**3. REPORT TYPE AND DATES COVERED** Master's Thesis	
4. TITLE AND SUBTITLE: Shipboard Radio Frequency and Free Space Optics Communications System using an Airborne Relay			**5. FUNDING NUMBERS**
6. AUTHOR(S) Kenneth W. St. Germain			
7. PERFORMING ORGANIZATION NAME(S) AND ADDRESS(ES) Naval Postgraduate School Monterey, CA 93943-5000			**8. PERFORMING ORGANIZATION REPORT NUMBER**
9. SPONSORING /MONITORING AGENCY NAME(S) AND ADDRESS(ES) N/A			**10. SPONSORING/MONITORING AGENCY REPORT NUMBER**
11. SUPPLEMENTARY NOTES The views expressed in this thesis are those of the author and do not reflect the official policy or position of the Department of Defense or the U.S. Government.			
12a. DISTRIBUTION / AVAILABILITY STATEMENT Approved for public release; distribution is unlimited			**12b. DISTRIBUTION CODE**

13. ABSTRACT (maximum 200 words)

This thesis explores the possible gains and discusses the constraints of a communications system that uses a ship to unmanned aerial vehicle (UAV) radio frequency (RF) link paired with a UAV to satellite free space optic (FSO) link to accomplish satellite communications. Analysis shows that a data rate of 2 gigabits per second (Gbps) with a $1 \cdot 10^{-6}$ probability of bit error can be attained by a shipboard system with a relatively small antenna and power supply if an FSO-enabled UAV is used. An experiment demonstrated that the addition of an FSO link and additional routing does not reduce the performance of a slower data rate RF link. The findings indicate that a composite RF and FSO ship-UAV-satellite system can be used within the Transformational Communications Architecture (TCA) and with the Navy's FORCEnet to enable network-centric operations (NCO).

14. SUBJECT TERMS Free space optics, FSO, airborne communications node, transformational communications architecture, TCA, network-centric operations, NCO, network centric warfare, NCW			**15. NUMBER OF PAGES** 101
			16. PRICE CODE
17. SECURITY CLASSIFICATION OF REPORT Unclassified	**18. SECURITY CLASSIFICATION OF THIS PAGE** Unclassified	**19. SECURITY CLASSIFICATION OF ABSTRACT** Unclassified	**20. LIMITATION OF ABSTRACT** UL

NSN 7540-01-280-5500 Standard Form 298 (Rev. 2-89)
Prescribed by ANSI Std. 239-18

THIS PAGE INTENTIONALLY LEFT BLANK

Approved for public release, distribution is unlimited

SHIPBOARD RADIO FREQUENCY AND FREE SPACE OPTICS COMMUNICATIONS SYSTEM USING AN AIRBORNE RELAY

Kenneth W. St. Germain
Lieutenant, United States Navy
BSEE, University of Nebraska-Lincoln, 2000

Submitted in partial fulfillment of the
requirements for the degree of

MASTER OF SCIENCE IN ELECTRICAL ENGINEERING

from the

NAVAL POSTGRADUATE SCHOOL
September 2005

Author: Kenneth W. St. Germain

Approved by: Frank Kragh
Thesis Advisor

Tri Ha
Second Reader

Jeffrey B. Knorr
Chairman, Department of Electrical and Computer Engineering

THIS PAGE INTENTIONALLY LEFT BLANK

ABSTRACT

This thesis explores the possible gains and discusses the constraints of a communications system that uses a ship to unmanned aerial vehicle (UAV) radio frequency (RF) link paired with a UAV to satellite free space optic (FSO) link to accomplish satellite communications. Analysis shows that a data rate of 2 gigabits per second (Gbps) with a $1 \cdot 10^{-6}$ probability of bit error can be attained by a shipboard system with a relatively small antenna and power supply if an FSO-enabled UAV is used. An experiment demonstrated that the addition of an FSO link and additional routing does not reduce the performance of a slower data rate RF link. The findings indicate that a composite RF and FSO ship-UAV-satellite system can be used within the Transformational Communications Architecture (TCA) and with the Navy's FORCEnet to enable network-centric operations (NCO).

THIS PAGE INTENTIONALLY LEFT BLANK

TABLE OF CONTENTS

I. INTRODUCTION....1
A. THESIS FOCUS....2
B. THESIS ORGANIZATION....2
II. NETWORK CENTRIC OPERATIONS....3
A. TRANSFORMATIONAL COMMUNICATIONS ARCHITECTURE....3
B. FORCENET....4
C. CHAPTER SUMMARY....5
III. LINK BUDGET....7
A. RECEIVER....7
B. NOISE....7
C. GAIN....8
1. Transmit Gain....9
2. Receiver Gain....10
D. LOSS....11
1. Free Space Loss....11
2. Attenuation....11
a. Scattering....11
b. Absorption....12
3. Turbulence....12
a. Beam Wander....13
b. Scintillation....13
c. Beam Spread....13
4. Pointing Loss....13
E. CHAPTER SUMMARY....14
IV. ANALYSIS....15
A. DATA RATE....16
B. FREQUENCY....16
C. TRANSMITTER AND RECEIVER....16
D. LOSSES....18
1. Free Space Loss....18
2. Atmospheric Loss....19
3. Pointing Loss....26
E. MODULATION....26
F. NOISE....27
G. BER PERFORMANCE....29
H. LINK EQUATION....32
I. CHAPTER SUMMARY....36
V. UAV SELECTION....37
A. REQUIREMENTS FOR A UAV RELAY....37
1. Payload....37

2. Loiter Time 40
3. Altitude 40
4. Deployability 41
B. TYPES OF UAVS 42
1. Fixed Wing 42
a. Predator B 42
b. Global Hawk 45
c. Helios 47
2. VTOL 49
3. Lighter than Air 50
a. 420K Aerostat 50
b. Aerosphere Airship 51
C. CHAPTER SUMMARY 53

VI. EXPERIMENT 55
A. SET UP 55
B. NETWORK CONFIGURATION 58
C. RESULTS 63
D. CHAPTER SUMMARY 73

VII. CONCLUSION AND FUTURE WORK 75
A. CONCLUSION 75
B. FUTURE WORK 75

LIST OF REFERENCES 77

INITIAL DISTRIBUTION LIST 81

LIST OF FIGURES

Figure 1. Transformational Communications Architecture (From [6]) 4
Figure 2. FORCEnet, the U.S. Navy's implementation of Network Centric Warfare (From [7])....5
Figure 3. Telescope designs (After [20])....10
Figure 4. Wavefront quality measured by Strehl Ratio versus altitude for several speeds (From [20])....12
Figure 6. Terabeam Elliptica Alignment and Monitoring Tool. 18
Figure 7. Ground to satellite (0.005 km to 35786 km) 7-9 GHz, directly overhead orientation, maritime aerosol environment. 20
Figure 8. Ground to satellite (0.005 km to 35786 km) 7-9 GHz, 20 degree angle from horizon, maritime aerosol environment 21
Figure 9. Ground to UAV (0.005 km to 19.8 km) 7-9 GHz, directly overhead orientation, maritime aerosol environment. 21
Figure 10. Ground to UAV (0.005 km to 19.8 km) 7-9 GHz, 20 degree angle from horizon, maritime aerosol environment. 22
Figure 11. UAV to satellite (19.8 km to 35786 km) 1500-1600 nm, directly overhead orientation, maritime aerosol environment. 23
Figure 12. UAV to satellite (19.8 km to 35786 km) 1500-1600 nm, 20 degree angle from horizon, maritime aerosol environment. 23
Figure 13. UAV to satellite (0.005 km to 35786 km) 1500-1600 nm, directly overhead orientation, maritime aerosol environment. 24
Figure 14. UAV to satellite (0.005 km to 35786 km) 1500-1600 nm, 20 degree angle from horizon, maritime aerosol environment. 24
Figure 15. UAV to satellite (0.005 km to 35786 km) 1500-1600 nm, directly overhead orientation, maritime aerosol environment. 25
Figure 16. UAV to satellite (0.005 km to 35786 km) 1500-1600 nm, 20 degree angle from horizon, maritime aerosol environment. 25
Figure 17. 8-PSK signal constellation (After [9]). 26
Figure 18. 8-PSK Bit Error Rate vs E_b/N_0 in an AWGN channel....30
Figure 19. Optical OOK bit error rate vs Signal Count in an AWGN channel....31
Figure 20. Beamsteering Mirrors in the Terabeam Elliptica 7421i....39
Figure 21. Cloud Types and Their Position in the Atmosphere (From [20])....41
Figure 22. General Atomics' Predator B, Altair Variant Flying as the Mariner (From [39])....43
Figure 23. Internal detail of Mariner BAMS proposal (From [39])....43
Figure 24. Global Hawk Mission Concept (From [40])....45
Figure 25. Global Hawk Cutaway (From [40])....46
Figure 26. Global Hawk at Beale Air Force Base (From [40])....47
Figure 27. Helios Prototype in July 2001 (From [41])....48
Figure 28. A-160 Hummingbird Illustration (From [42]) 49
Figure 29. Lockheed Martin 420K Aerostat (From [44]) 51
Figure 30. Footprint of TechSphere's Aerosphere (From [46])....52

Figure 31. Hewlett Packard h6315 iPAQs, Dell i9300 and Terabeam Elliptica 7421i.....56
Figure 32. Experiment set up with RF link in the foreground 57
Figure 33. Elliptica 7421i Ethernet connection.....58
Figure 34. Diagram of entire network showing IP addresses.....59
Figure 35. USS Essex communicating to USS Chancellorsville in Trident Warrior 03 (After [53]).....60
Figure 36. iPAQ 192.168.0.15 61
Figure 37. iPAQ 192.168.0.10 61
Figure 38. Both iPAQs transmit to i9300.....61
Figure 39. iPAQ 192.168.0.10 62
Figure 40. iPAQ 192.168.0.10 62
Figure 41. iPAQ 192.168.0.15 sends to i5150 64
Figure 42. iPAQ 192.168.0.15 sends to i9300 64
Figure 43. iPAQ 192.168.0.10 sends to i5150 65
Figure 44. iPAQ 192.168.0.10 sends to i9300 65
Figure 45. Both iPAQs transmit to the i5150 at the same time.....66
Figure 46. Total summary of both iPAQs transmitting to i5150 at the same time 67
Figure 47. Both iPAQs transmit to i9300 at the same time.....67
Figure 48. Total summary of both iPAQs transmitting to i9300 at the same time 68
Figure 49. iPAQ 192.168.0.10 sends to i5150, using 192.168.0.15 as a relay, while 192.168.0.15 does not send.....69
Figure 50. iPAQ 192.168.0.10 sends to i9300, using 192.168.0.15 as a relay, while 192.168.0.15 does not send.....69
Figure 51. Both iPAQs transmit to i5150, and 192.168.0.15 acts as a relay.....70
Figure 52. Total summary of both iPAQs transmitting to the i5150, while 192.168.0.15 acts as a relay 71
Figure 53. Both iPAQs transmit to i9300, and 192.168.0.15 acts as a relay.....72
Figure 54. Total summary of both iPAQs transmitting to the i9300, while 192.168.0.15 acts as a relay 73

LIST OF TABLES

Table 1. DSCS III Ship to Satellite Link Budget for 2 Mbps Data Rate (After [29]) ...32
Table 2. Ship to UAV RF Link Budget for 2 Gbps Data Rate 33
Table 3. Elliptica 7421i UAV to Satellite FSO Link Budget for 2 Gbps Data Rate.....35
Table 4. UAV Payload weight and power requirements 40
Table 5. Specifications for Predator B, Mariner Variant (After [39]) 44
Table 6. Specifications for Global Hawk, RQ-4A (After [40]) 46
Table 7. Specifications for Helios (After [41]).....48
Table 8. Specifications for A-160 Hummingbird (From [42]) 50
Table 9. Specifications for Lockheed Martin 420K (After [44]).....51
Table 10. Specifications for Techsphere's Aerosphere (After [47]).....52
Table 11. Weather conditions at the Monterey Airport on August 24, 2005 (After [50]).....55
Table 12. IP and Hardware address for devices used 58

THIS PAGE INTENTIONALLY LEFT BLANK

ACKNOWLEDGMENTS

First and foremost, I would like to thank my wife, Andi, for her love and support during our time here in Monterey. Her ceaseless motivation and the energy in all she pursues are truly inspirational. I would also like to thank Professor Frank Kragh for agreeing to be my advisor. His insight, technical guidance, and encouraging support have made accomplishing this research a reality. Without the assistance of Professor Don Walters, the quality of this thesis would have greatly suffered. The Cryptologic Research Lab at the Naval Postgraduate School has been an invaluable resource for which the author is extremely grateful.

My sincere appreciation goes to SPAWAR Systems Center San Diego, whose financial support made the purchase of equipment and supplies for the experiment possible.

THIS PAGE INTENTIONALLY LEFT BLANK

EXECUTIVE SUMMARY

The need for high data rate communications has increased dramatically from Operation Desert Storm in 1991 to Operation Enduring Freedom and Operation Iraqi Freedom in 2003 [1]. A variety of enabling technologies and supporting communication architectures are being developed to meet this ever increasing requirement. The overall result of these undertakings will increase shared awareness of the battlespace and make network-centric operations possible.

Free space optics (FSO) is an attractive technology for high data rate communication. FSO provides greater bandwidth, smaller beam divergence angles, and smaller antennas than traditional microwave links. This yields a potential for higher data rate across the link and lowers the probability that an adversary can intercept it. A drawback to using FSO on the earth's surface is the attenuation caused by the atmosphere. Molecules and particles in the atmosphere attenuate electromagnetic radiation to varying degrees through scattering and absorption. Thick clouds and fog drastically reduce the transmission of optical frequencies, making FSO unreliable if it is to be used in all weather conditions. The attenuation effects can be reduced by increasing the altitude of the FSO link to the thinner upper atmosphere or space.

In order to communicate reliably to terrestrial units in all weather conditions, a radio frequency (RF) link is needed. Since RF links do not degrade through clouds or foliage as much as FSO links, and link margin increases when the path distance decreases, using a UAV as a relay allows increased data rate and allows FSO transmission to a satellite. In this scheme, the benefits of FSO are realized and the disadvantages are mitigated.

This proposed relay system offers a practical means to include mobile ships and ground units within the TCA. By providing these users with large amounts of bandwidth, NCO and FORCEnet are enabled, thus making Sea Power 21 realizable. This thesis explores the possible gains and discusses the constraints of a ship-UAV-satellite communications system. Analysis specifies that a data rate of 2 Gbps with a $1 \cdot 10^{-6}$ probability of bit error can be attained with a relatively small antenna and power supply if

an FSO-enabled UAV is used. An experiment demonstrated that the addition of an FSO link and additional routing did not reduce the performance of a slower data rate RF link.

I. INTRODUCTION

The ability to create a shared awareness for all war fighters and decision makers whether during peacetime, crisis, or war, is a key advantage for a military force. The wide variety of user platforms, mobility requirements, and service and coalition differences make communication, let alone high speed data transfer, a nontrivial task. Real-time command and control and the capability to provide actionable intelligence from a remote headquarters to tactical units on the front lines could be a tremendous benefit in any conflict. [2]

Satellite communication systems allow wireless global contact and collaboration. Deployed naval, airborne, and expeditionary ground forces use satellite links in order to communicate and to receive and transmit information. Unfortunately, the capacity of these links is limited in data rate as well as the number of users who can access them. In a large regional conflict, the accessible satellites in the area become a high demand asset. This congestion restricts users' high data rate reach back communication. A priority system allocates satellite resources and connectivity to users. [3]

In order to help alleviate the demand on these satellite channels and provide users at all echelons in the battlespace with shared awareness, several enabling technologies are being investigated and implemented. Some of these include high bandwidth free space optic (FSO) links among satellites and manned and unmanned airborne units, Internet Protocol (IP) based communication that can be dynamically routed, and mobile, radio frequency (RF) terminals that are reduced in size but provide higher data rate than currently available. A system that can take advantage of these technologies is an RF link between a ship and an airborne node that routes the traffic to a satellite using an FSO link. The airborne node in this proposed communications system functions as a communication relay and could be unmanned. Instead of the current ship-satellite architecture, the ship-UAV-satellite architecture allows routing of traffic at an intermediary position and requires conversion between RF and FSO. If the communication is meant for a unit that is also within view of the UAV, the UAV will relay the transmission without using the satellite link, creating a ship-UAV-ship

architecture. This enables high data rate communication without placing additional burden on the satellite.

A. THESIS FOCUS

The focus of this thesis will be to determine possible data rate improvements, user antenna size reductions, and parameter constraints of the composite RF and FSO system compared to that of a traditional RF satellite communications link. Technology and systems currently in operational use or available commercially will be discussed and compared where available.

For convenience, this thesis specifies a ship terminal in the ship-UAV-satellite construct. However, the concepts are equally applicable to a ground vehicle, an aircraft, or man-portable radio system. Analysis would need to be performed for the new parameters.

B. THESIS ORGANIZATION

Chapter II of this thesis defines network-centric operations and the implementation of network-centric warfare.

Chapter III identifies factors within the ship-UAV-satellite communication system that will determine the data rate and performance of the link.

Chapter IV is an analysis of the link using parameters from Chapter III. A ship-satellite link budget is compared with the ship-UAV-satellite link budget.

Chapter V is a discussion of specific types of UAVs currently in operation or under development. Based on the UAV limitations and the communication link requirements, suitable candidates were nominated.

Chapter VI describes an experiment using IEEE 802.11b devices in concert with a FSO link.

Chapter VII summarizes the findings in the thesis and provides recommendations for further work.

II. NETWORK CENTRIC OPERATIONS

The tenets of network-centric warfare (NCW) propose that a robustly networked force can increase mission effectiveness through collaboration that is facilitated by a shared situational awareness accomplished by information sharing. Network-centric operations (NCO) describe the military application of the tenets and governing principles of NCW during peacetime, crisis and war. NCO help to increase combat power by enhancing command and control through global situational awareness. [2]

Studies conducted on the use of NCO in real-world operations show that capabilities are improved and that some operations are not possible without a well networked force. In order to attain this networked force, there must be an implementation of NCW across the combined spectrum of military services and coalition partners. This chapter briefly presents two mutually supportive communications architectures that allow for the implementation of NCW. [2]

A. TRANSFORMATIONAL COMMUNICATIONS ARCHITECTURE

The Transformational Communications Architecture (TCA) offers a communications infrastructure that links interoperable and independent systems across the DoD, the Intelligence Community, and the National Aeronautics and Space Administration. It is a dynamic transport mechanism that enables NCO and supports the transformational visions of U.S. military forces. Enhancing command and control and mission effectiveness is accomplished in part by increasing decision maker mobility, and allowing for the sharing of quality information which reduces operational risk [2]. The TCA provides increased access and data capacity to deployed and mobile users through the use of an internet of space, airborne, and ground networks. By fully implementing Internet Protocol across the TCA, and through the support of multi-level security, the end-to-end connectivity to a variety of users enables global information sharing. Ground, air, sea, and space assets will all be capable of generating, processing, receiving, or routing information [4]. The TCA employs Advanced Extremely High Frequency satellites as well as satellite cross-links using laser communication to realize protected, survivable communication. Figure 1 shows a depiction of the TCA. [5]

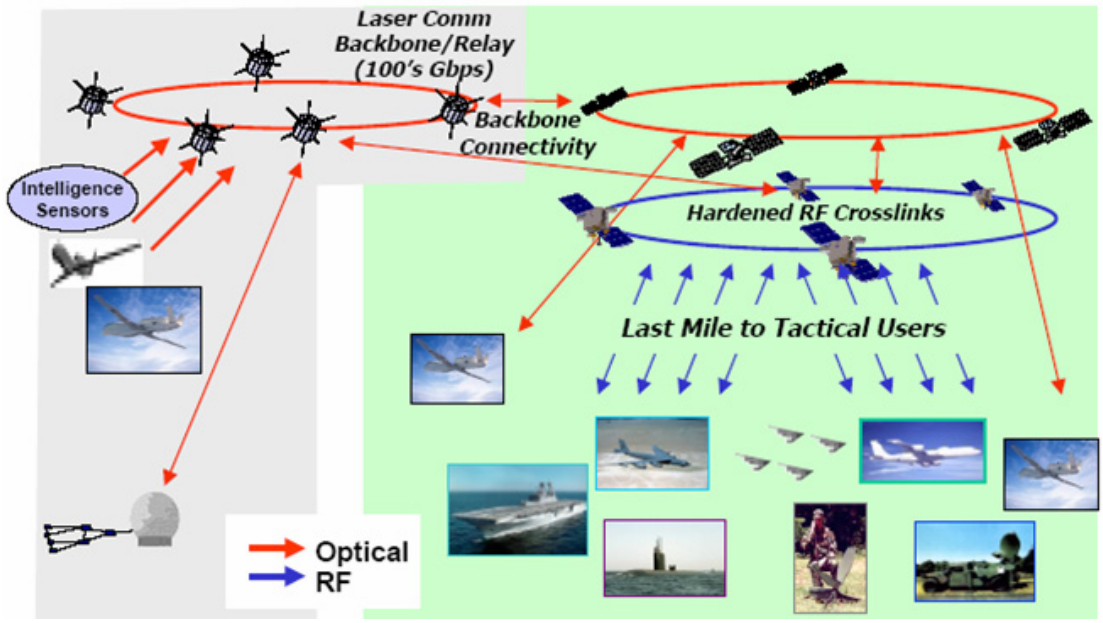

Figure 1. Transformational Communications Architecture (From [6])

In an operational context, the TCA allows time sensitive information to be relayed from sensors to shooters and decision makers. This creates shared battlespace awareness. The TCA provides the war fighter with continuous accessibility to airborne and space assets, allowing the military to employ network-centric operations, and increase combat power. As shown in Figure 1, unmanned aircraft are envisioned to transmit information to the space segment using optical links. The addition of an RF link from the UAV to the tactical user could reduce the demand for satellite access, alleviating possible congestion. [4]

B. FORCENET

FORCEnet is the name for the U.S. Navy's integrating concept and framework that allows the Navy to implement NCW in the information age. Figure 2 depicts the Navy's vision for FORCEnet.

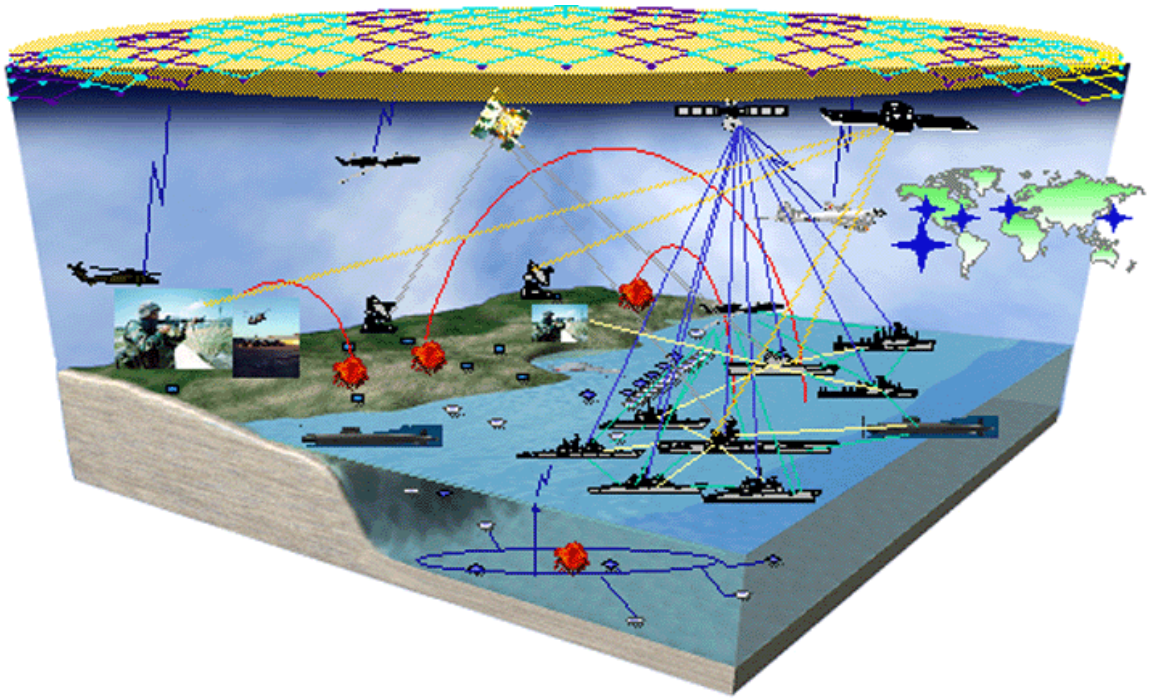

Figure 2. FORCEnet, the U.S. Navy's implementation of Network Centric Warfare (From [7])

By connecting the Navy's war fighters, sensors, networks, and platforms, to each other through FORCEnet and the TCA, there is an increase in combat effectiveness. This is accomplished through an improved shared awareness of the battlespace and faster, more accurate decision making, which leads to better execution. [8]

Since the FORCEnet-enabled Navy will be able to take advantage of the benefits of NCO through the TCA, the ship-UAV-satellite link has the potential to be an integral component of the maritime communication suite. In addition to large deck ships, the high data rate associated with optical communication could be leveraged by small ships and Special Forces, provided the size of the RF user terminal can be minimized.

C. CHAPTER SUMMARY

There are many areas of research and technology involved with the TCA and FORCEnet. These include, but are not limited to, laser communications, packet based multiple-access, antennas for communication on the move, and high capacity RF links [5]. The Navy's transformation and development of FORCEnet will have the capacity to

allow information sharing with joint, multiagency, and coalition partners [8]. A ship-UAV-satellite link could support both FORCEnet and the TCA.

In the next chapter, the factors that comprise the ship-UAV-satellite communications link budget are presented. Relevant parameters in the analysis of the link margin are taken from current operational and commercial systems when available.

III. LINK BUDGET

Analysis of a communications system traditionally involves development of a link budget. Parameters of a communications link can be analyzed to predict performance and show the constraints of the transmitter, receiver, and the channel.

Working in decibels, the amount of signal power received is given by $(P_r)_{\text{dBW}} = (P_t)_{\text{dBW}} + (G_t)_{\text{dB}} + (G_r)_{\text{dB}} - (L_s)_{\text{dB}} - (L_a)_{\text{dB}}$. Where P_t is the power transmitted, G_t is the gain of the transmitter, G_r is the gain of the receiver, L_s is the free space loss, and L_a are additional losses encountered, such as atmospheric and pointing losses. Transmit power and the gain of the transmitter are often combined as a single term and denoted as the effective isotropic radiated power (EIRP). This is written as $(EIRP)_{\text{dBW}} = (P_t)_{\text{dBW}} + (G_t)_{\text{dB}}$. [9]

A. RECEIVER

A receiver can be designed to operate in a given environment with acceptable bit error rate (BER) performance if a specified signal to noise ratio is met. This received signal is provided by the transmitter and is diminished by the channel and non-ideal components within the receiver. The receiver cannot be designed for a noiseless environment and be expected to operate in a real world situation, so a minimum signal to noise ratio for operation must be specified and then achieved.

B. NOISE

Noise is introduced at the receiver by several sources. In RF communications, the dominant noise source is usually Johnson noise, also known as, thermal noise, while quantum noise becomes dominant in FSO [10].

The expression for thermal noise power in a bandwidth B in the RF band is, $N = kTB$, where k is Boltzmann's constant, $1.38 \cdot 10^{-23}$ $\text{W} \cdot \text{s} / \text{K}$, and T is the noise temperature (in Kelvin). Thermal noise is always present, in varying degrees, because it is dependent on the temperature viewed by the receiver in addition to noise temperatures of electronic devices in the receiver [9]. Thermal noise has a relatively flat and frequency independent power density across the spectrum from DC up to about 10^{12} Hz [9]. Since

even the furthest reaches of deep space are above absolute zero [11], there will always be a thermal noise component in this range of frequencies. The one-sided power spectral density for thermal noise is only frequency independent for $kT >> hf$, and is approximated from $N(f) = \frac{hf}{e^{hf/kT} - 1} + hf$, where h is Planck's constant, $6.6261 \cdot 10^{-34}\ \mathrm{J \cdot s}$, and f is the frequency of the electromagnetic radiation [12]. In RF systems, the detection of signals in thermal noise and other electronic circuitry classically involves an additive Gaussian model [13]. The random signal is represented as the sum of a Gaussian noise random variable and signal [14].

When dealing with near-optical frequencies, thermal noise can be neglected due to the high frequencies used [10]. The noise terms for FSO systems are shot noise processes involving the quantum noise, and dark current noise [13]. The random arrival of photons creates shot noise that is modeled by a Poisson process. Quantum noise is expressed as $N_Q = hfB$ [15]. Dark current is the name for the process where electrons are emitted from the photodetector even when there is no incident light and add directly to the average detector output [16]. In the optical band, noise is frequency dependent, placing a limit on the performance of the detector. It cannot be represented purely as a sum of signal and additive noise since the signal itself has an associated variance [16]. Besides thermal noise, the analysis on the optical system will also neglect saturation, and photomultiplier effects, following Gagliardi and Karp [17].

C. GAIN

Gain can be used at the transmitter as well as the receiver to boost the magnitude of the signal through the use of a directive antenna [14]. This reduces the power the transmitter requires and/or increases the minimum amount of signal power received through the channel. Antennas may be designed to collect more signal power than the isotropic antenna. Doing so means balancing directivity with potential power accumulated. A large amount of power can be collected in one direction, but at the cost of not being able to collect as much power from another. Directivity can be advantageous especially in the case where potential interference may exist from other nearby sources. Outside of the antenna's main beam, other signals are attenuated. By the

same token, if a signal is transmitted between misaligned directional antennas, pointing losses arise. In ground to satellite RF links, the losses are typically only a few tenths of a decibel. [18]

Ideal antenna gain for a circular aperture of area A is given by $G_{ideal} = \frac{4\pi A}{\lambda^2}$, for both RF and laser communications [19]. By comparing this optimum case, it is straightforward to see that the antenna gain for FSO systems has the potential to be several orders of magnitude greater than RF gain by virtue of the $1/\lambda^2$ factor. An optical antenna with a five inch aperture operating at 1550 nm has an ideal gain of 108 dB, where a 100 ft microwave antenna operating at 8 GHz has a 68 dB gain. The optical antenna, in this case, has a 40 dB advantage, ten-thousand times the gain, despite its smaller dimensions.

1. Transmit Gain

A parabolic antenna is often used to direct RF power in a given direction and increasing the size of the dish increases the gain for a given transmission frequency. Antenna gain for a parabolic antenna is given by $G_{t,RF} = \eta \cdot G_{ideal} = \eta \frac{4\pi A}{\lambda^2}$, where η is the aperture efficiency factor typically between 0.5 and 0.6, λ is the wavelength of the signal, and A is the area of the antenna [9].

FSO antennas can be conventional telescopes that often have obstructions in the center of the lens. Figure 3 shows various telescope designs.

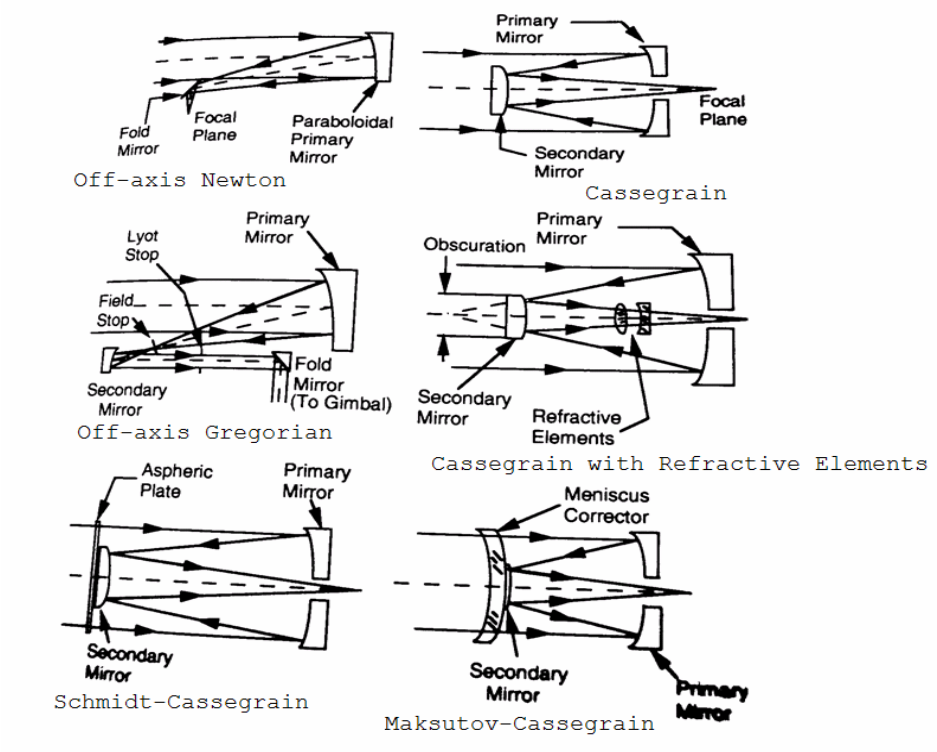

Figure 3. Telescope designs (After [20]).

The transmit gain has an efficiency factor, that accounts for losses caused by obscurations such as blockage and other losses. If we restrict analysis to the far field, the expression for the gain of a circular transmitter antenna becomes $G_{t,FSO} = \frac{4\pi A}{\lambda^2} \cdot \left[\frac{2}{\alpha^2} \left[e^{-\alpha^2} - e^{-\gamma^2 \alpha^2} \right]^2 \right]$ [20]. α is the ratio of antenna radius to beam width at the $1/e^2$ intensity point, γ is the obscuration ratio, b/a, where b is the radius of the center lens obstruction and a is the radius of the outer aperture. The optimum transmitter efficiency with no obscurations, only on-axis gain, and far field transmission is 0.8145 [19].

2. Receiver Gain

The antenna gain for the receiver in RF systems is identical to the transmitter gain, $G_{r,RF} = \eta \frac{4\pi A}{\lambda^2}$ [9]. However, the gain for the circular receive antenna in laser communications is different than its transmit antenna counterpart. The receiver gain is

expressed as $G_{r,FSO} = \frac{4\pi A}{\lambda^2} \cdot (1-\gamma)^2$. It is clear that if obscurations are minimized, the antenna gain approaches the ideal. [21]

A key parameter in characterizing the receiving system performance is G_r/T, a combination of the receiver antenna gain and the system noise temperature. The signal to noise ratio of a satellite link can be used to predict how well the link will operate. Using the G_r/T term, the link equation for signal to noise ratio becomes $\left(\frac{P_r}{P_n}\right)_{\text{dB}} = (\text{EIRP})_{\text{dBW}} + (G_r/T)_{\text{dB/K}} - (L_s)_{\text{dB}} - (L_a)_{\text{dB}} - (k)_{\text{dBJ/K}} - (B)_{\text{dBHz}}$. [18]

D. LOSS

Losses in a communications system come from several sources. Some significant losses are caused by the distance between the transmitter and receiver, molecule and aerosol attenuation, atmospheric turbulence, and pointing losses. [16]

1. Free Space Loss

Free space losses, $L_s = \left(\frac{4\pi d}{\lambda}\right)^2$, occur as the transmitted radiation is spread out over a spatial volume and is proportional to the square of the distance the signal travels, d [9]. The free space loss is often the largest loss component [14].

2. Attenuation

Attenuation in the channel due to absorption and scattering is given by the transmission loss factor, $L_t = e^{-\mu d}$, where μ is the sum of the absorption and scattering attenuation parameters [16]. Whether a signal will be scattered or absorbed by molecules and aerosols in the channel is dependent on the signal's wavelength as well as the size and attenuation coefficient of the particle [20].

a. Scattering

Scattering describes the behavior of light as it reflects and bounces through the atmosphere. The amount of received energy is attenuated as it propagates. Rayleigh scattering occurs with particles or molecules smaller than the wavelength of the transmitted energy. This type of scattering affects shorter wavelengths like those in the

visible spectrum much more than the larger RF and infrared wavelengths. Mie scattering describes interactions with particles about the same size of the transmitted wavelength. [22]

b. Absorption

Absorption by molecules and particles in the atmosphere is dependent on the frequency of the transmitted radiation and the amount of absorbing substance in the channel. The atmosphere contains oxygen, water vapor, and carbon dioxide, but the frequency of the transmission determines to what degree each substance will absorb the energy [22]. Because of the abundance of oxygen and water vapor in the lower atmosphere, high frequency signal attenuation due to scattering and absorption are much larger near the Earth's surface than at high altitudes. [20]

3. Turbulence

As light travels across a path, it may be bent or refracted when it crosses into different densities of atmosphere. Especially across large distances in the atmosphere, pockets of different temperature and indexes of refraction exist. This can cause beam wander, scintillation, and beam spreading. A turbulent boundary layer can be caused by air flowing over an aircraft's exterior, distorting the phase. This effect is measured by the Strehl ratio, which can be minimized by maintaining high altitude and slow speed as show in Figure 4. [20]

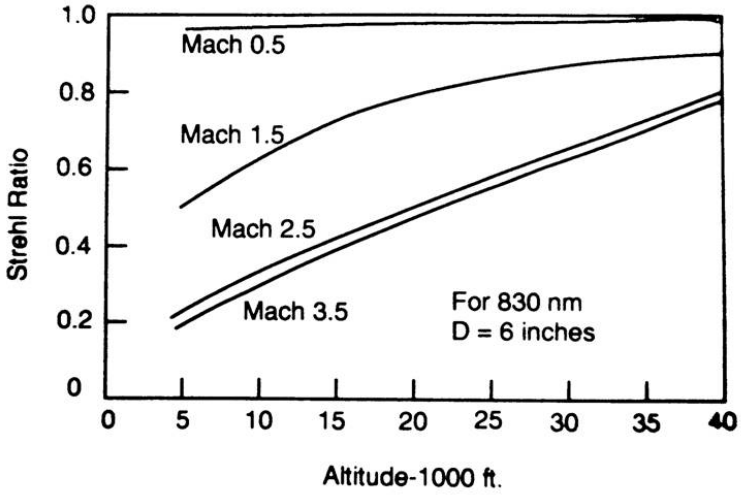

Figure 4. Wavefront quality measured by Strehl Ratio versus altitude for several speeds (From [20])

a. Beam Wander

Beam wander describes the effect of a relatively narrow beam passing through a large pocket and slightly altering its course [16]. These fluctuations are typically slow and can be minimized by using a tracking system [20].

b. Scintillation

FSO communication systems are adversely influenced by scintillation's rapidly changing random fluctuations, especially near the Earth's surface. Small temperature variations cause constructive and destructive interference. The difference in index of refraction from points in the channel can be modeled in a time varying probabilistic manner. Examples of environments where scintillation is likely to be easily observed are on a hot road, the desert sand, or the deck of a ship. [20]

c. Beam Spread

A turbulent channel can cause the divergence of a beam to increase larger than predicted [23]. Beam divergence occurs in free space and is given as $\theta_{div} = \frac{2\lambda}{\pi \cdot a}$, where θ_{div} is the angle in radians that a plane wave spreads from leaving an aperture of radius a [20]. Beam spread has a weak dependence on wavelength, and with laser systems, adaptive optics can be used to mitigate this effect [24].

4. Pointing Loss

Pointing losses occur when the transmit and receive antennas are misaligned so that the full antenna gain is not realized. In some cases, the transmitter or receiver antenna directivity may be so high that failing to align them carefully will prevent successful transmission. In the case of transmitters and receivers with highly directional antennas, a mechanism for tracking must be employed to ensure that pointing losses are minimized. The narrow beam width of optical systems provide for excellent communications security from a low probability of intercept view, but the tracking requirements must be held to a much higher specification when compared to microwave systems. Pointing losses in RF ground to satellite systems may be quite small and beam divergence may be large enough that a fine tracking system is not required. However, even in great distance inter-satellite links, laser communication beam divergence is so

small that pointing errors are significant to bit error rate and overall link performance [20]. Where pointing losses do exist, this thesis will model them as an additional loss, increasing the L_a term. [18]

E. CHAPTER SUMMARY

The design of a communications link requires knowledge of the constraints of the system. Losses and gain are partially dependent on the frequency band of the system and figure prominently in the final signal to noise ratio achieved at the receiver. By careful analysis of the factors that benefit and degrade the signal, a prediction can be made as to whether the system will meet the required data rate and performance specifications. If the expected criteria are not met, changes to the system under design must be made. These changes can include processing modifications such as the use of forward error correction coding, and hardware substitutions such as replacing antennas and oscillators.

Next, link budget analysis and comparison of an RF ship-satellite link to a composite link using RF from ship to UAV and FSO from UAV to satellite will be made. When available, parameters of systems currently in use will be applied. Through this analysis, the possibility and potential benefits of using the ship-UAV-satellite architecture will be discussed.

IV. ANALYSIS

The link analysis for a ship-satellite communications system can be compared to that of a ship-UAV-satellite system. In the latter case, the ship-UAV link will be RF, and the UAV-satellite link will be optical. Both cases will be analyzed using estimated parameters for systems that are currently in use or have the potential to be fielded with technology that is available today.

In both cases, the satellite will be in a geosynchronous orbit with an altitude of 35,786 km. This is the distance from the satellite to a position on the earth directly below the satellite. The slant range from a transmitter on the earth's surface to the satellite is approximated by the range of a geostationary orbit as $d = \sqrt{R_E^2 + a_{GSO}^2 - 2R_E \cdot a_{GSO} \cdot \sin\left[b + \sin^{-1}\left(\frac{R_E}{a_{GSO}} \cdot \cos(b)\right)\right]}$, where R_E is the radius of the earth, a_{GSO} is the radius of the circular orbit from the center of the earth, and b is the elevation angle of the earth station. For purposes of illustration through this chapter, an elevation angle of $b = 20$ degrees and a slant range of d = 40,000 km are assumed. [25]

The RF link between the ship and the satellite as well as the RF link between the ship and the UAV will use an SHF system that employs the WSC-6 (V)9 antenna group. The ship to satellite will use the WSC-6 (V)9 radio group and use DSCS III parameters. This system is currently employed on small combatant and support ships in the U.S. Navy and provides up to 2.048 Mbits/s data rate per channel [26].

The optical link will be based on a system that can support a very high data rate. From the constraints dictated by the data rate and BER performance, a candidate system will be prescribed. The UAV will be at an altitude of 65,000 ft, or 19.8 km. Again, it is expected that the user may be in a location other than directly underneath the UAV, so the furthest range will be 58 km, corresponding to approximately a 20 degree angle up from the horizon.

A. DATA RATE

In order to rationalize the added complexity of using a FSO-mounted UAV for communications, the data rate realized should be much greater than the rate currently obtained only using RF. If the resulting data rate from the ship-UAV-satellite link is several orders of magnitude more than currently obtained, it may receive more consideration than a modest increase. Therefore, we will attempt a data rate of 2 Gbps per channel between the ship and satellite, using the UAV as a relay.

Although the ship's antenna group can remain the same, it is expected that the RF radio group on the ship and UAV will be different from the current satellite configuration. The antenna group on the UAV may also need to be altered depending on the constraints of the airframe. The goal in configuring the new ship-UAV RF system will be to increase the data rate and the link margin from the ship-satellite system. With the additional link margin, it will be shown that the system can be changed to increase the data rate from the original 2Mbps, improve the BER performance, reduce the size of the ship's antenna, reduce the required power, or any combination of these.

B. FREQUENCY

The WSC-6 (V)9 operates in the X-band when communicating with the DSCS. The receive frequency band and wavelengths are 7.25-7.75 GHz and 3.87-4.14 cm, while the transmit band is 7.9-8.4 GHz and 3.57-3.79 cm [26].

The FSO system will operate in the infrared portion of the spectrum at the eye-safe wavelength of 1550nm. This corresponds to a frequency of 193.5 THz.

C. TRANSMITTER AND RECEIVER

The antenna for the WSC-6 (V)9 is 1.52 m in diameter, and the EIRP is given as 95.3 dBm, and while receiving, $G/T = 16.4$ dB/K [27]. The antenna gain can be calculated assuming an illumination efficiency factor of 0.6 to be $G_{t,RF} = \eta \frac{4\pi A}{\lambda^2} = 0.6 \cdot \frac{4\pi\left(1.81\ \text{m}^2\right)}{\left(4 \cdot 10^{-2}\ \text{m}\right)^2} = 8551 = 39\ \text{dB}$. The DSCS III satellite has an EIRP of 70 dBm [28] with a G/T of -1 dB/K [29]. This corresponds to the main beam antenna aboard the DSCS III satellite that has a diameter of 45 in. [29]. The transmit

gain for this antenna is $G_{t,RF} = 0.6 \cdot \frac{4\pi\left(1.02\ \text{m}^2\right)}{\left(3.68 \cdot 10^{-2}\ \text{m}\right)^2} = 5682.8 = 37.5\ \text{dB}$. The RF antenna on the UAV will be selected in order to provide the necessary proposed data rate at the BER performance specified while meeting the size and weight requirements necessary to be mounted to the UAV selected. The UAV should be capable of serving all ships in line of sight, and would require a multi-beam RF antenna, possibly using a phased array. In order to simplify the analysis for this thesis, a conventional parabolic RF antenna serving one ship at a time is used.

The physical characteristics of the transmitters used in the FSO segment will be modeled from the Terabeam Elliptica 7421i. The Elliptica is a commercially available FSO transceiver for use in extending or connecting local or wide area computer networks [30]. The aperture of the Elliptica is about 10 cm in diameter, as shown in Figure 5.

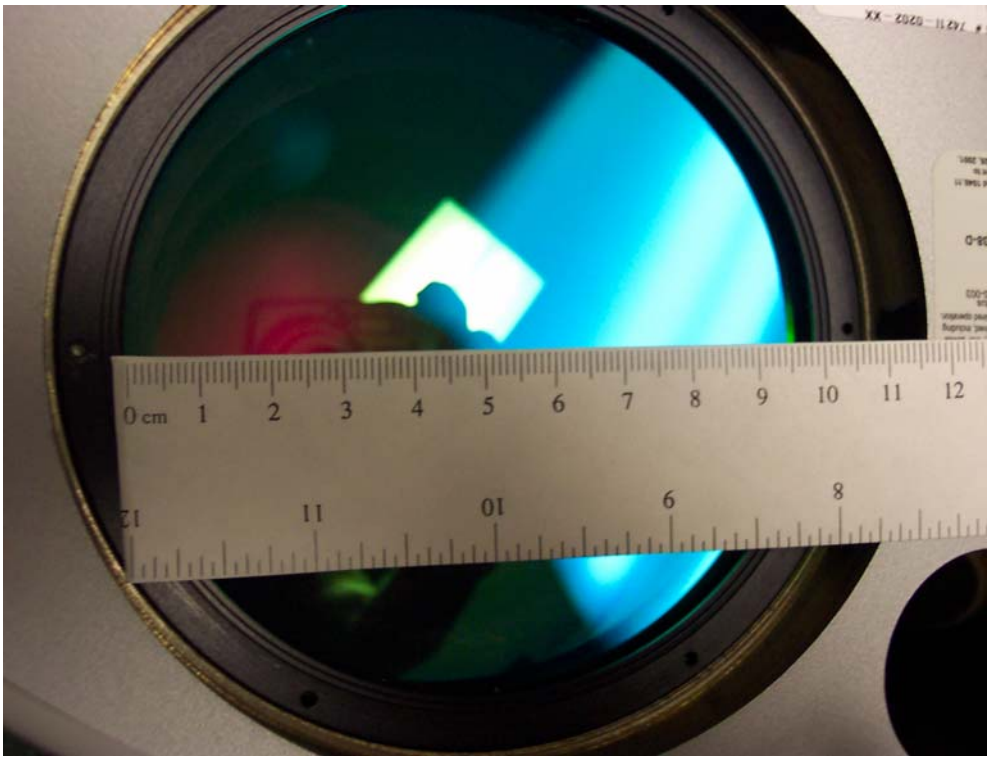

Figure 5. Terabeam Elliptica Aperture.

When the link is active, the alignment and monitor software tool in Figure 6 shows that the transmitted power is about 15 mW.

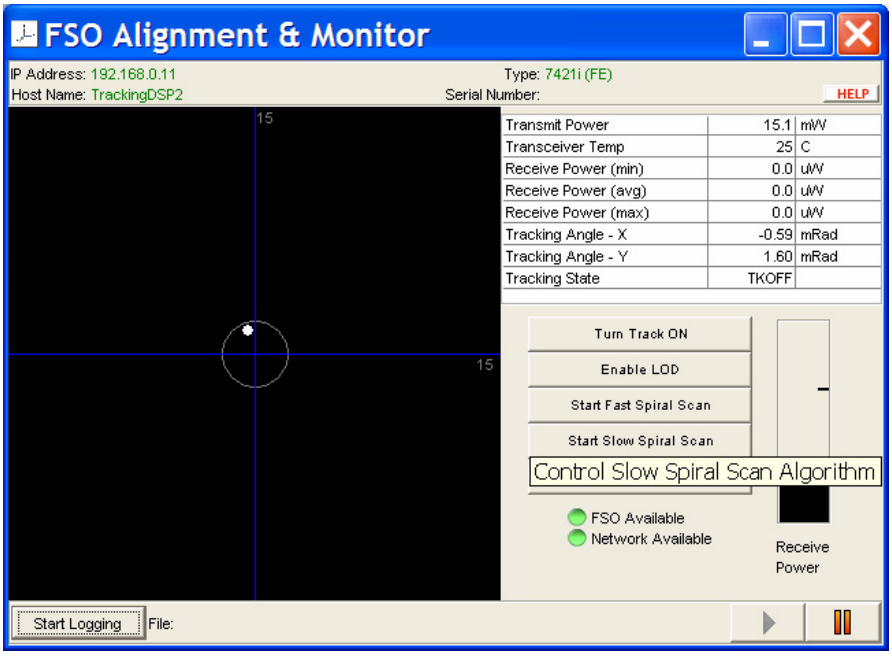

Figure 6. Terabeam Elliptica Alignment and Monitoring Tool.

Assuming on-axis gain and minimizing truncation effects, the FSO transmitter has

$$\begin{aligned} \text{EIRP} &= P_t \cdot G_{t,FSO} = P_t \cdot \frac{4\pi A}{\lambda^2} \cdot \left[\frac{2}{\alpha^2} \left[e^{-\alpha^2} - e^{-\gamma^2 \alpha^2} \right]^2 \right] \\ &= P_t \cdot \frac{4\pi^2 a^2}{\lambda^2} 0.81 = 15 \text{ mW} \cdot \frac{4\pi^2 \cdot \left(5 \cdot 10^{-2} \text{ m}\right)^2}{\left(1550 \cdot 10^{-9} \text{ m}\right)^2} \cdot 0.81 \\ &= 4.99 \cdot 10^{11} \text{ mW} = 117 \text{ dBm} \end{aligned} \tag{4.1}$$

D. LOSSES

From the transmitter to the receiver, the signal is degraded from many sources. Some losses are inevitable but the degree of attenuation may be dependent on the wavelength of the transmitted signal.

1. Free Space Loss

Although both link designs have the same overall distance, spanning from the ship to the satellite, the free space losses are different because of the wavelength term. The free space loss on the uplink and downlink between the ship and satellite are

$$L_{s,ship-sat} = \left(\frac{4\pi d}{\lambda}\right)^2 = \left(\frac{4\pi \cdot 40000 \cdot 10^3 \text{ m}}{4 \cdot 10^{-2} \text{ m}}\right)^2 \quad (4.2)$$
$$= 1.58 \cdot 10^{20} = 202 \text{ dB}$$

$$L_{s,sat-ship} = \left(\frac{4\pi d}{\lambda}\right)^2 = \left(\frac{4\pi \cdot 40000 \cdot 10^3 \text{ m}}{3.68 \cdot 10^{-2} \text{ m}}\right)^2 \quad (4.3)$$
$$= 1.86 \cdot 10^{20} = 202.7 \text{ dB}$$

The loss on the uplink and downlink between the ship and UAV in the RF band as well as loss between the UAV and satellite at FSO frequencies are

$$L_{s,ship-UAV} = \left(\frac{4\pi d}{\lambda}\right)^2 = \left(\frac{4\pi \cdot 58 \cdot 10^3 \text{ m}}{4 \cdot 10^{-2} \text{ m}}\right)^2 \quad (4.4)$$
$$= 3.31 \cdot 10^{14} = 145.2 \text{ dB}$$

$$L_{s,UAV-ship} = \left(\frac{4\pi d}{\lambda}\right)^2 = \left(\frac{4\pi \cdot 58 \cdot 10^3 \text{ m}}{3.68 \cdot 10^{-2} \text{m}}\right)^2 \quad (4.5)$$
$$= 3.89 \cdot 10^{14} = 145.9 \text{ dB}$$

$$L_{s,UAV-sat} = L_{s,sat-UAV} = \left(\frac{4\pi d}{\lambda}\right)^2$$
$$= \left(\frac{4\pi \cdot (40000 - 19.8) \cdot 10^3 \text{ m}}{1550 \cdot 10^{-9} \text{ m}}\right)^2 = 1.05 \cdot 10^{29} \quad (4.6)$$
$$= 290.2 \text{ dB}$$

2. Atmospheric Loss

The absorption and scattering losses can be approximated through the use of PLEXUS. The Air Force Research Laboratory, Space Vehicles Directorate has developed PLEXUS (Phillips Laboratory EXpert-assisted User Software), a software program that allows the user to predict the transmittance of the electromagnetic spectrum through the atmosphere. Spectral transmittance, the fraction of electromagnetic radiation transmitted through a medium is given by Beer's Law as $\tau = \frac{S_{out}(f)}{S_{in}(f)}$, where $S_{in}(f)$ and

$S_{out}(f)$ are the input and output power spectral densities, respectively [31]. PLEXUS can model several environmental situations including the link geometry, time of day, time of year, visibility, cloud types, and aerosol conditions in order to forecast and plot probable interactions and transmittance. [32]

To show how different conditions can alter the atmospheric loss, Figures 7 through 12 show how PLEXUS models attenuation. The figures illustrate clear conditions with good visibility (5 km) as well as foggy with poor visibility (0.5 km) either in a directly overhead geometry or at a 20 degree angle up from the horizon. Figures 7 through 10 illustrate the spectral transmittance for RF links while Figures 11 through 16 illustrate the spectral transmittance for optical links.

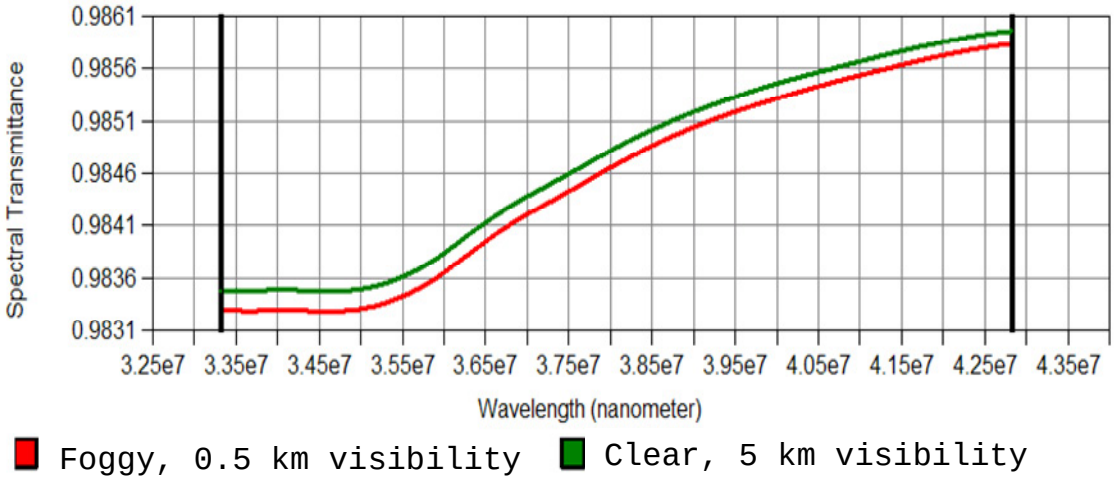

Figure 7. Ground to satellite (0.005 km to 35786 km) 7-9 GHz, directly overhead orientation, maritime aerosol environment.

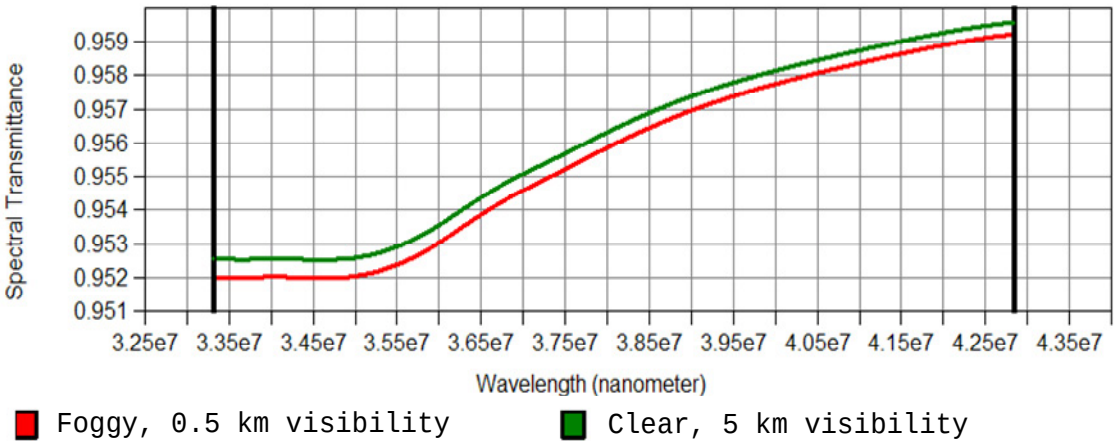

Figure 8. Ground to satellite (0.005 km to 35786 km) 7-9 GHz, 20 degree angle from horizon, maritime aerosol environment

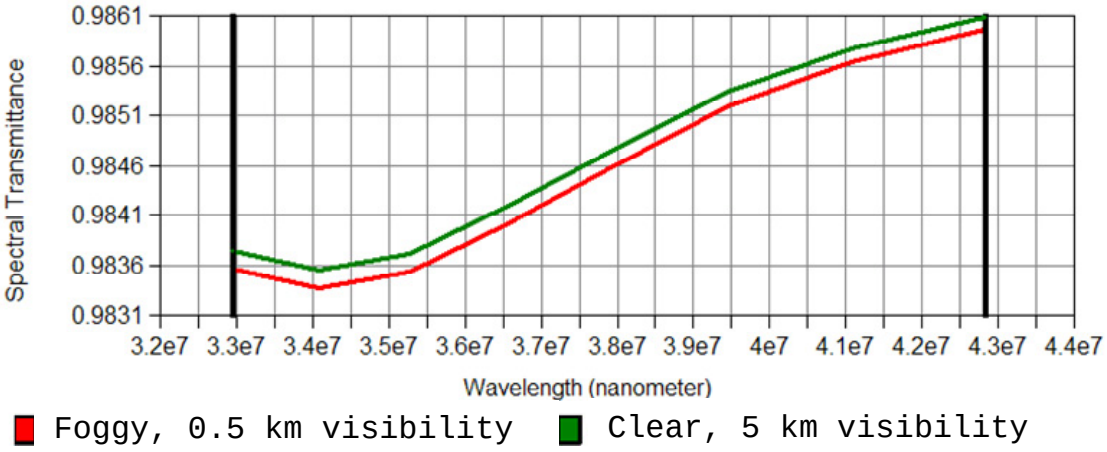

Figure 9. Ground to UAV (0.005 km to 19.8 km) 7-9 GHz, directly overhead orientation, maritime aerosol environment.

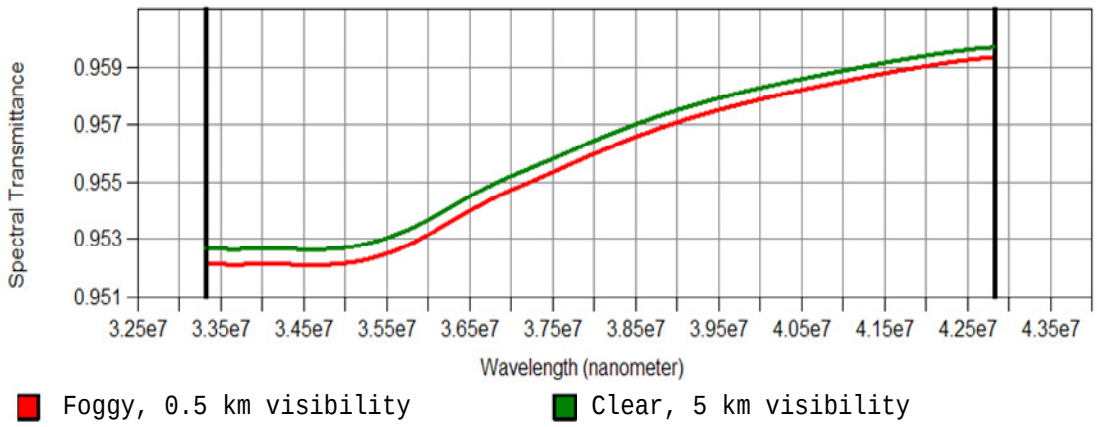

Figure 10. Ground to UAV (0.005 km to 19.8 km) 7-9 GHz, 20 degree angle from horizon, maritime aerosol environment.

By examining the figures, it is clear that atmospheric attenuation in the 7-9 GHz frequency band occurs mostly in the altitudes below 19.8 km, since the higher altitude of 35786 km has hardly any effect compared to the 19.8 km altitude. Attenuation is more pronounced when the angle of transmission is not directly overhead. When transmitting straight up, the signal effectively passes through the least amount of atmosphere. Regardless, the losses due to absorption for RF are very low. In fact, the atmospheric loss for the RF link in the worst case scenario of a low transmission angle through fog for either ground to satellite or ground to UAV is approximately, $L_{atm,RF} \approx 1/0.95 = 0.2dB$.

The following figures show the atmospheric attenuation for the FSO link.

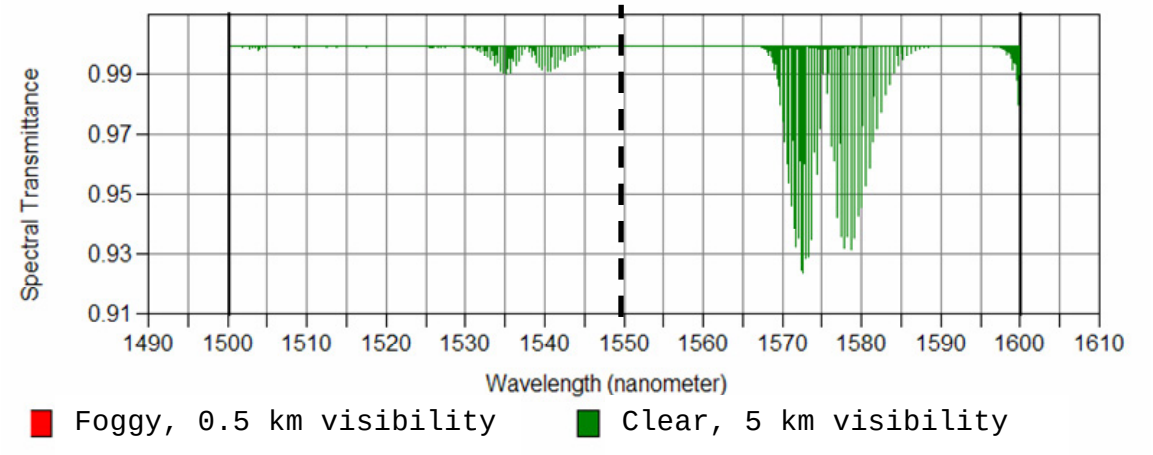

Figure 11. UAV to satellite (19.8 km to 35786 km) 1500-1600 nm, directly overhead orientation, maritime aerosol environment.

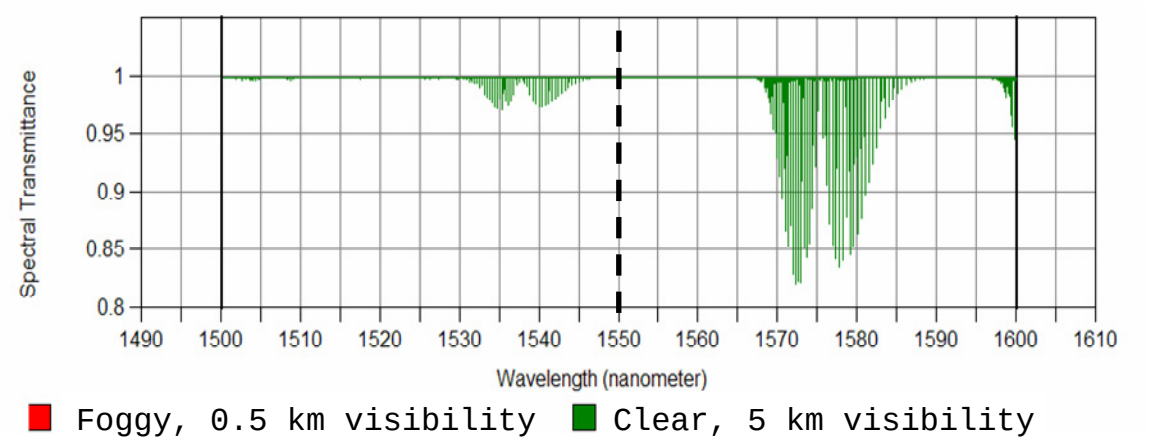

Figure 12. UAV to satellite (19.8 km to 35786 km) 1500-1600 nm, 20 degree angle from horizon, maritime aerosol environment.

In Figures 11 and 12, the UAV is positioned above the fog layer, so there is no difference in transmittance due to fog near the earth's surface. The only absorption and scattering indicated in these figures occurs at altitudes higher than 19.8 km. At this altitude, at the 1550 nm wavelength, there are virtually no atmospheric losses for the optical link. At 1572 nm, the atmospheric attenuation is significantly increased when the UAV and satellite geometry is changed from directly overhead to a 20 degree angle.

To illustrate the effect that the lower atmosphere has on laser communications, the altitude of the UAV is reduced to a level as if it were mounted on a ship's mast in clear and foggy conditions. Clear conditions with different orientations are shown in Figures 13 and 14. Figures 15 and 16 show these orientations with fog.

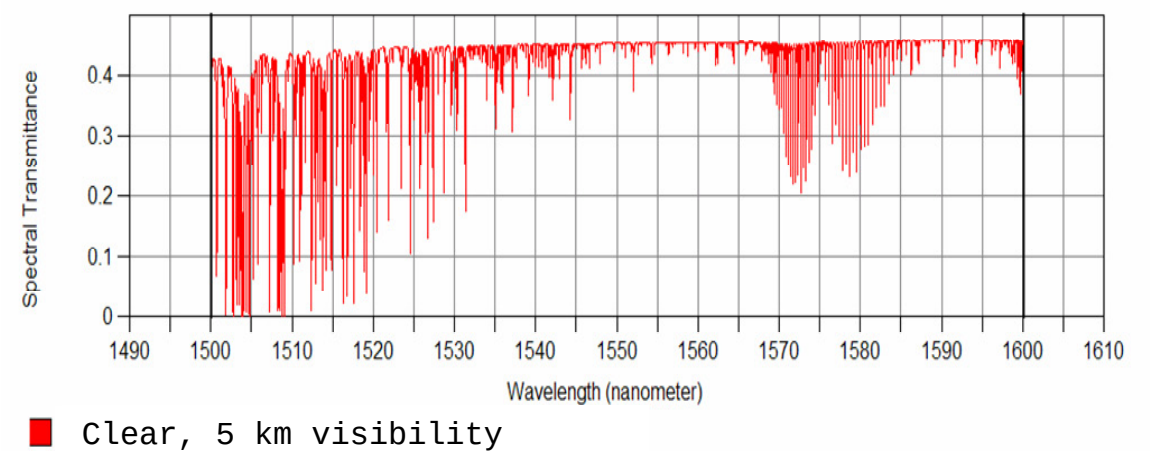

Figure 13. UAV to satellite (0.005 km to 35786 km) 1500-1600 nm, directly overhead orientation, maritime aerosol environment.

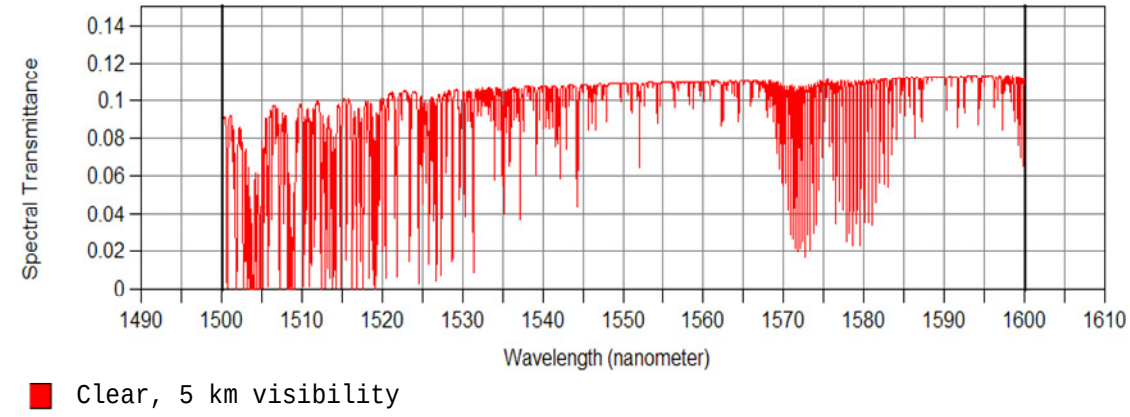

Figure 14. UAV to satellite (0.005 km to 35786 km) 1500-1600 nm, 20 degree angle from horizon, maritime aerosol environment.

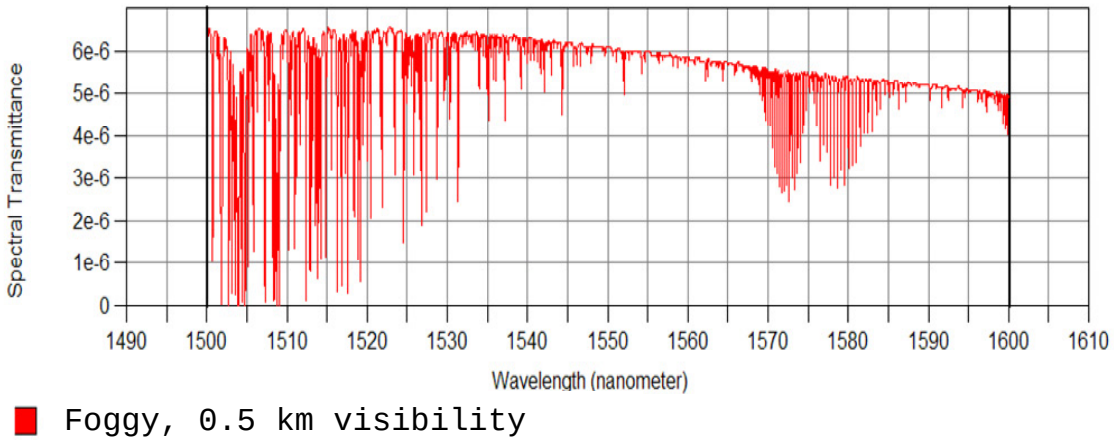

Figure 15. UAV to satellite (0.005 km to 35786 km) 1500-1600 nm, directly overhead orientation, maritime aerosol environment.

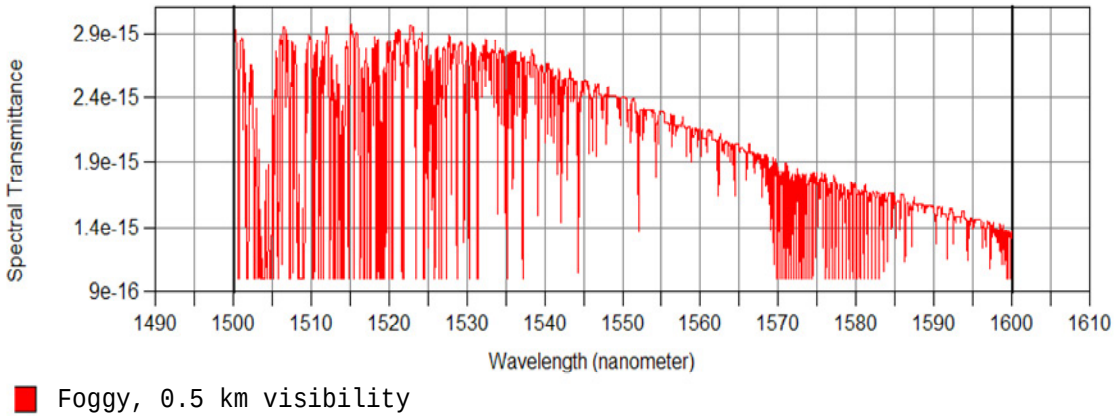

Figure 16. UAV to satellite (0.005 km to 35786 km) 1500-1600 nm, 20 degree angle from horizon, maritime aerosol environment.

Figure 13 shows a large attenuation compared to any of the RF transmissions or the FSO transmission at 19.8 km. With a 20 degree angle as shown in Figure 14, the loss at 1550 nm in clear conditions is almost 10 dB. This is worse than the RF case, but the loss is not so extreme that it could not be overcome by increasing the transmission power or raising the antenna gain through increasing the size of the antenna aperture. However, to compensate for the loss due to fog shown in Figure 16, the increase in antenna size or transmission power would be unacceptably large. This motivates the research of using RF at the lower altitudes between the ship and the UAV, and FSO between the UAV and the satellite.

3. Pointing Loss

The pointing loss for the ground to satellite RF link is included in the G/T term of -1 dB/K [29]. If the UAV selected is large enough, and can be reasonably expected to accommodate the 45 in. DSCS III antenna, the same G/T term may be applied for the ship to UAV RF link.

For the FSO link, the pointing loss will be approximated following Lambert and Casey to be 2.4 dB. This error takes into consideration tracking errors as well as alignment and point-ahead accuracy shortcomings inherent in a mobile architecture such as this. [20]

E. MODULATION

The WSC-6 (V)9 can use phase shift keying with eight symbols (8-PSK) to modulate the data [27]. The signal constellation for 8-PSK is shown in Figure 17, where each point represents a symbol representing three bits of information. Ideally, instead of bits being sent one at a time, bandwidth is conserved and three bits are transmitted per transmission. If rectangular pulses are assumed, then using the null-to-null bandwidth, W, the bandwidth efficiency for 8-PSK modulation is $\frac{R}{W} = \frac{R}{2R_s} = \frac{R}{2 \cdot R/3} = 1.5$, where R is the bit rate and R_s is the symbol rate. [9]

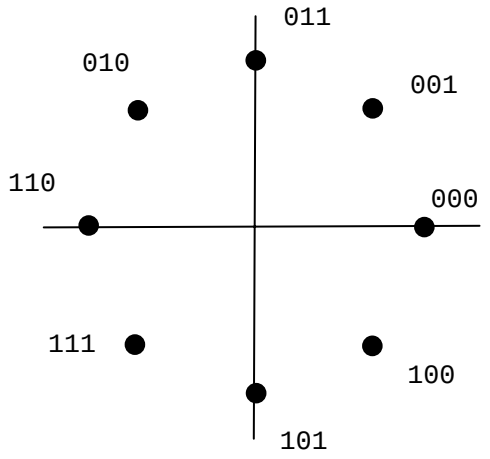

Figure 17. 8-PSK signal constellation (After [9]).

For the FSO link, there are several options for the type of signal detection and modulation used. One of the simplest and most common techniques used is direct detection with binary baseband signaling. Direct detection involves converting optical energy to electrical energy by the detector and does not require any mixing of the incident signal. Electrons are released from a photodetector when it is illuminated by incident radiation. [16]

Binary ones and zeros can be sent across the link by On-off keying (OOK). The bandwidth efficiency for OOK is $\frac{R}{W} = \frac{1}{2}$, where W is the null to null bandwidth of the OOK signal and R is the data rate in bits per second. [33]. This modulation requires 4 GHz of bandwidth at a 2 Gbps data rate. There are other modulation schemes available at better performance and spectral efficiency, but at a higher complexity cost.

F. NOISE

The receive noise temperature for the DSCS III satellite is 832.5 K [29], while the receive noise temperature for the WSC-6 (V)9 is 169.8 K [27]. Receiver G/T is given for the DSCS III as -1 dB/K [29], while the WSC-(V)9 has a G/T 16.4 dB/K [27]. Since the WSC-6 (V)9 can use an 8-PSK modem, and the bandwidth is one two-thirds of the bit rate, B will be 1.365 MHz at 2.048 Mbps, or 1.333 GHz at 2 Gbps. For purposes of this thesis, the noise temperature for the ship to UAV link will be the same as for the ship to DSCS III link. Noise power at the receiver for the uplink and downlink are

$$\begin{aligned} N_{ship-sat} &= kT_uB = \left(1.38\cdot10^{-23}\ \text{J/K}\right)\left(832.5\ \text{K}\right)\left(1.365\cdot10^{6}\ \text{Hz}\right) \\ &= 1.57\cdot10^{-14}\ \text{W} = -138\ \text{dBW} \end{aligned} \tag{4.7}$$

$$\begin{aligned} N_{sat-ship} &= kT_dB = \left(1.38\cdot10^{-23}\ \text{J/K}\right)\left(169.8\ \text{K}\right)\left(1.365\cdot10^{6}\ \text{Hz}\right) \\ &= 3.2\cdot10^{-15}\ \text{W} = -145\ \text{dBW} \end{aligned} \tag{4.8}$$

$$\begin{aligned} N_{ship-UAV} &= kT_dB = \left(1.38\cdot10^{-23}\ \text{J/K}\right)\left(832.5\ \text{K}\right)\left(1.333\cdot10^{9}\ \text{Hz}\right) \\ &= 1.53\cdot10^{-11}\ \text{W} = -108\ \text{dBW} \end{aligned} \tag{4.9}$$

$$N_{UAV-ship} = kT_uB = \left(1.38\cdot10^{-23}\,\text{J/K}\right)\left(169.8\,\text{K}\right)\left(1.333\cdot10^{9}\ \text{Hz}\right)$$
$$= 3.12\cdot10^{-12}\ \text{W} = -115\ \text{dBW} \quad (4.10)$$

The quantum noise in the optical system is given by

$$N_Q = hfB = \left(6.63\cdot10^{-34}\,\text{J}\cdot\text{s}\right)\cdot\left(193\cdot10^{12}\,\text{Hz}\right)\cdot\left(4\cdot10^{9}\,\text{Hz}\right)$$
$$= 5.12\cdot10^{-10}\ \text{W} = \text{-92.9 dBW} \quad (4.11)$$

The dark current noise is dependent on the average dark current of the individual photodetector. The Elliptica FSO system does not disclose the dark current for its infrared InGaAs avalanche photodiode detector. For this, we follow Einarsson and use an average dark current, i_d, of $1.5\cdot10^{-9}$ A [13]. When a zero is transmitted, ideally, there are no photons transmitted. The average number of electrons counted during the bit interval $[0,t]$ when a zero is transmitted will be the average noise count, m_0, where $m_0 = \int_0^t \left(\frac{i_d}{q}\right)dt$. When a one is transmitted, the average number of electrons counted in the bit interval will be m_1, where $m_1 = \int_0^t \left(\frac{\eta_q \cdot P_r}{hf} + \frac{i_d}{q}\right)dt$, and η_q is the quantum efficiency defined to be the probability of an electron being released for an incident photon [16]. Again following Einarsson, η_q will be 0.9. At 2 Gbps, t is $5\cdot10^{-10}$ s, and

$$m_0 = \int_0^t \left(\frac{i_d}{q}\right)dt = \int_0^{5\cdot10^{-10}\text{s}} \left(\frac{1.5\cdot10^{-9}\ \text{A}}{1.6\cdot10^{-19}\ \text{C}}\right)dt$$
$$= \left(9.38\cdot10^{9}\ \text{electrons}/\text{s}\right)\cdot\left(5\cdot10^{-10}\text{s}\right) = 4.69\ \text{electrons} \quad (4.12)$$

$$
\begin{aligned}
m_1 &= \int_0^t \left(\frac{\eta_q \cdot P_r}{hf} + \frac{i_d}{q} \right) dt \\
&= \int_0^{5\cdot10^{-10}\,\mathrm{s}} \left(\frac{0.9 \cdot P_r}{\left(6.63\cdot10^{-34}\,\mathrm{J\cdot s}\right)\left(193\cdot10^{12}\ \mathrm{Hz}\right)} \right) dt + 4.69 \text{ electrons} \qquad (4.13) \\
&= P_r \cdot \left(3.51\cdot10^{9}\ \text{electrons}/\mathrm{W}\right) + 4.69 \text{ electrons}
\end{aligned}
$$

For m_0 and most likely for m_1, we do not compute an integer for the number of electrons. Instead of rounding them up or down, we will use these average values to determine the optimum threshold for signal detection when we calculate the probability of bit error. At that time an integer value for the threshold will be assigned. [13]

G. BER PERFORMANCE

The performance of both systems will be held to a probability of bit error less than $1\cdot10^{-6}$. In order to maintain the performance threshold for the 8-PSK modulation scheme in the RF systems, a minimum received signal to noise ratio must be achieved. In the FSO system, a minimum signal count for a given noise count over the bit interval must be met.

The BER for 8-PSK can be written in terms of energy per bit, E_b as

$$
P_{b,RF,8PSK} \approx \frac{2Q\left(\sqrt{\frac{2E_b \log_2 8}{N_0}} \sin\frac{\pi}{8}\right)}{\log_2 8} = \frac{2}{3} Q\left(\sqrt{\frac{E_b}{N_0}} 0.94\right) \text{ [9]} \qquad (4.14)
$$

The received power is related to energy per bit by $P_r = E_b \cdot R_b$. The BER versus E_b/N_0 for 8-PSK is shown in Figure 18.

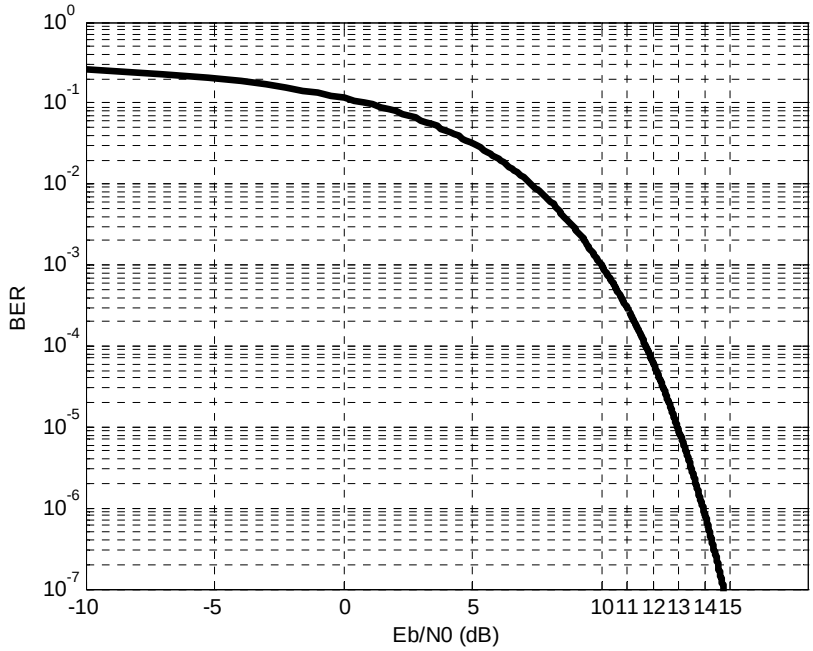

Figure 18. 8-PSK Bit Error Rate vs E_b/N_0 in an AWGN channel

From Figure 18, it can be seen that in order to maintain a BER of less than $1 \cdot 10^{-6}$, E_b/N_0 must be greater than 14 dB. From this graph, and the relationship of received power to energy per bit and bit rate, we see at a given received power, the performance level can be maintained by adjusting the bit rate. For P_r held constant, and a specified BER, if E_b/N_0 is not large enough, the bit rate must be decreased, and likewise for a very large E_b/N_0, the bit rate can be increased. [14]

The minimum value of E_b/N_0 is for the overall satellite link, including the uplink and the downlink. Typically in a ground to satellite link, the downlink limits the entire system due to the limited EIRP available from the satellite. The overall E_b/N_0 is calculated from the overall signal to noise ratio, $\frac{S}{N}$, more conveniently expressed as the sum of uplink and downlink noise to signal ratios, $\frac{N}{S} = \left(\frac{N}{P_r}\right)_U + \left(\frac{N}{P_r}\right)_D$. Then, we relate the overall signal to noise ratio to E_b/N_0 as $\frac{E_b}{N_0} = \frac{S}{N}\left(\frac{W}{R_b}\right)$. [14]

The probability of bit error for an optical system using OOK is given as

$$P_{b,FSO,OOK} = \frac{1}{2}\sum_{n=\kappa_{\text{int}}+1}^{\infty}\frac{m_0^n}{n!}e^{-m_0} + \frac{1}{2}\sum_{n=0}^{\kappa_{\text{int}}}\frac{m_1^n}{n!}e^{-m_1} \text{ [13]} \tag{4.15}$$

The threshold for detection is given by $\kappa = \frac{m_1 - m_0}{\ln(m_1) - \ln(m_0)}$ [13]. Since we are dealing with discrete electrons, the threshold used is the integer portion, κ_{int}. There is also a Gaussian approximation for this error probability expressed as $P_{b,FSO,OOK} \approx Q\left(\sqrt{m_1} - \sqrt{m_0}\right)$ [13]. The BER for optical OOK is shown in Figure 19.

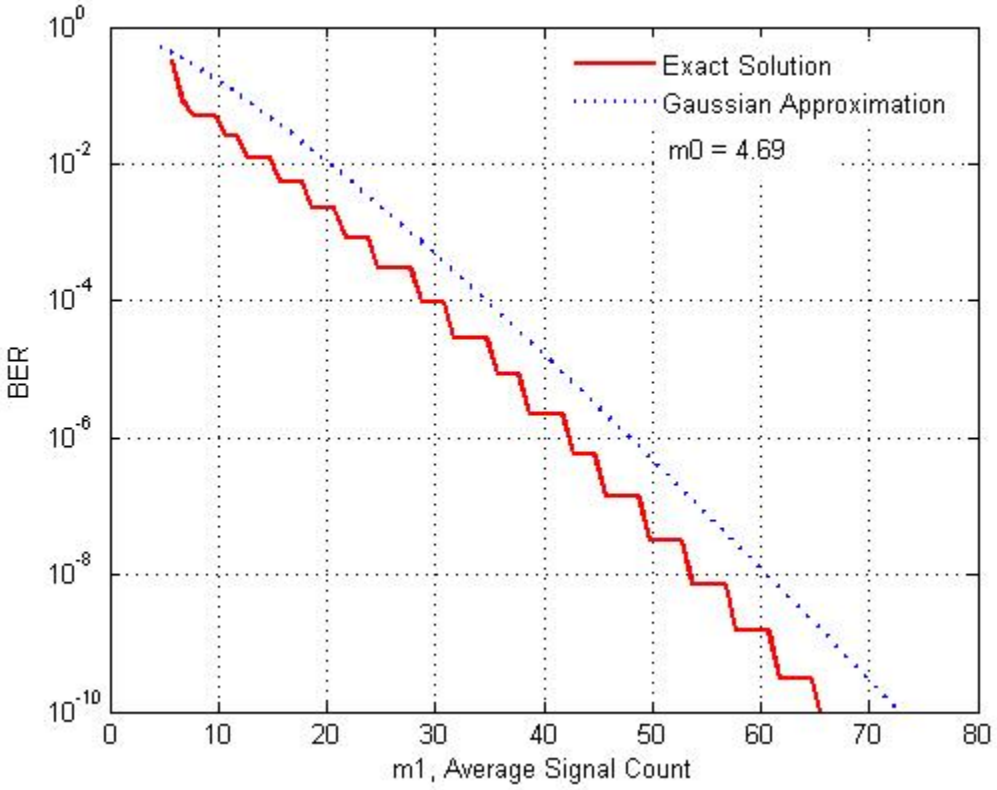

Figure 19. Optical OOK bit error rate vs Signal Count in an AWGN channel

In order to maintain the necessary BER performance, the photodetector of the receiver must generate at least 42 electrons within the bit period when illuminated with signal power. From earlier, we calculated the average number of signal electrons to be

$m_1 = P_r \cdot \left(3.51 \cdot 10^9 \text{ electrons}/\text{W}\right) + 4.69 \text{ electrons}$. Therefore the minimum received signal power for a one to be correctly detected is 0.11 nW or -69 dBm.

H. LINK EQUATION

With all the necessary terms identified for the analysis, the link budget can be calculated. The results for the ship to satellite link are shown in Table 1, while the ship to UAV link is shown in Table 2.

	Link Parameter	Value	Units	Comments
Uplink				
Ship to Satellite	Ship *EIRP*	65.3	dBW	
	Path Loss (7.5 GHz)	202	dB	
	Atmospheric Loss	0.2	dB	
	Satellite G/T	-1	dB/K	Includes pointing loss
	Boltzmann's Constant	-228.6	dBW/K-Hz	
	Bandwidth	61.3	dB-Hz	1.365 MHz
	Uplink Signal to Noise Ratio	29.4	dB	
Downlink				
Satellite to Ship	Satellite *EIRP*	44	dBW	
	Path Loss (8.15 GHz)	203	dB	
	Atmospheric Loss	0.2	dB	
	Ship G/T	16.4	dB/K	
	Boltzmann's Constant	-228.6	dBW/K-Hz	
	Bandwidth	61.3	dB-Hz	1.365 MHz
	Downlink Signal to Noise Ratio	24.5	dB	
Total	Signal to Noise (Total)	23.3	dB	
	Bandwidth	61.3	dB-Hz	
	Bit Rate	63	dB-bps	2Mbps
	E_b/N_0	21.58	dB	
	E_b/N_0 for $P_b \le 1 \cdot 10^{-6}$	14	dB	
	Margin	7.58	dB	

Table 1. DSCS III Ship to Satellite Link Budget for 2 Mbps Data Rate (After [29])

	Link Parameter	Value	Units	Comments
Uplink				
Ship to UAV	Ship *EIRP*	65.3	dBW	
	Path Loss (7.5 GHz)	145.2	dB	
	Atmospheric Loss	0.2	dB	
	UAV RF G/T	-1	dB/K	Includes pointing loss
	Boltzmann's Constant	-228.6	dBW/K-Hz	
	Bandwidth	91.25	dB-Hz	1.333 GHz
	Uplink Signal to Noise Ratio	56.25	dB	
Downlink				
UAV to Ship	UAV *EIRP*	44	dBW	
	Path Loss (8.15 GHz)	146	dB	
	Atmospheric Loss	0.2	dB	
	Ship G/T	16.4	dB/K	
	Boltzmann's Constant	-228.6	dBW/K-Hz	
	Bandwidth	91.25	dB-Hz	1.333 GHz
	Downlink Signal to Noise Ratio	51.55	dB	
Total	Signal to Noise (Total)	50.3	dB	
	Bandwidth	91.25	dB-Hz	
	Bit Rate	93	dB-bps	2 Gbps
	E_b/N_0	48.53	dB	
	E_b/N_0 for $P_b \leq 1 \cdot 10^{-6}$	14	dB	
	Margin	34.5	dB	

Table 2. Ship to UAV RF Link Budget for 2 Gbps Data Rate

As with the satellite link, a total signal to noise ratio is calculated in case the UAV acts like the satellite and relays the signal similar to the DSCS III scenario. It is possible that two ships are beyond line of sight from one another, but could communicate via the UAV. This would relieve the need for a satellite.

The link margin for the ship to UAV link with a 2 Gbps data rate is much more than the ship to satellite link with 2 Mbps. If the calculated margin for the DSCS III link is kept as the minimum margin to account for fading caused by heavy rain and smaller elevation angles, changes can be made to the system while still achieving the required

performance at the designated bit rate. The ship and the UAV's EIRP can be reduced so that the overall signal to noise ratio remains above 23.3 dB. Reducing EIRP is accomplished by decreasing the size of the antenna to yield a smaller gain, or by using less power to transmit. If the UAV remains the same, the EIRP of the ship can be calculated from

$$\left(\frac{S}{N}\right)_{\text{dB}} = -10\log\left(10^{-\frac{\left(\frac{S}{N}\right)_{UAV_{\text{dB}}}}{10}} + 10^{-\frac{\left(\frac{S}{N}\right)_{ship_{\text{dB}}}}{10}}\right) \quad [17]$$

$$\left(\frac{S}{N}\right)_{\text{dB}} = -10\log\left(10^{-\frac{(\text{EIRP}_{\text{UAV}})_{\text{dBW}} - (L_s)_{\text{dB}} - (L_a)_{\text{dB}} + \left(G/T_{ship}\right)_{\text{dB/K}} - (k)_{\text{dBW/K-Hz}} - (B)_{\text{dB-Hz}}}{10}} + 10^{-\frac{\left(\text{EIRP}_{\text{ship}}\right)_{\text{dBW}} - (L_s)_{\text{dB}} - (L_a)_{\text{dB}} + \left(G/T_{UAV}\right)_{\text{dB/K}} - (k)_{\text{dBW/K-Hz}} - (B)_{\text{dB-Hz}}}{10}}\right) \quad (4.16)$$

$$23.3\text{ dB} = -10\log\left(10^{-\frac{51.55\text{ dB}}{10}} + 10^{-\frac{(\text{EIRP}_{\text{ship}})_{\text{dBW}} - 9.05\text{ dB}}{10}}\right)$$

$$\text{EIRP}_{ship} = 32.35\text{ dBW}$$

The minimum EIRP of the ship is 32.35 dBW or 1718 W. With a transmitter power of 5 W, the minimum antenna radius, a becomes

$$\text{EIRP} = P_t \cdot G_{t,RF} = P_t \cdot \eta \frac{4\pi A}{\lambda^2}$$

$$1718\text{ W} = (5\text{ W}) \cdot 0.6 \cdot \frac{4\pi\left(\pi \cdot a^2\text{ m}^2\right)}{\left(4 \cdot 10^{-2}\text{ m}\right)^2} = 14804 \cdot a^2 \quad (4.17)$$

$$a = 0.15\text{ m}$$

This parabolic antenna is now a foot in diameter, requires only 5 W of power, and could be connected to a radio to attain a 2 Gbps data rate.

The link budget for the FSO link modeled from the Elliptica 7421i is shown in Table 3.

	Link Parameter	Value	Units
Uplink			
UAV to Satellite	UAV *EIRP*	117	dBm
	Path Loss (1550 nm)	290.2	dB
	Pointing Loss	2.4	dB
	Atmospheric Loss	0	dB
	Satellite Gain	105.2	dB
	Received Power	-70.4	dBm
	Required Received Power for $P_b \le 1 \cdot 10^{-6}$	-69	dBm
	Margin	-1.4	dB
Downlink			
Satellite to UAV	Satellite *EIRP*	117	dBm
	Path Loss (1550 nm)	290.2	dB
	Pointing Loss	2.4	dB
	Atmospheric Loss	0	dB
	UAV Gain	105.2	dB
	Received Power	-70.4	dBm
	Required Received Power for $P_b \le 1 \cdot 10^{-6}$	-69	dBm
	Margin	-1.4	dB

Table 3. Elliptica 7421i UAV to Satellite FSO Link Budget for 2 Gbps Data Rate

The link margin for this system is less than zero, which means the received power is insufficient for a 2 Gbps data rate with a BER of $1 \cdot 10^{-6}$. According to Sklar, systems employing new technologies often require additional margin compared to systems that have been built and tested many times over. Some of the INTELSAT systems have a 4 to 5 dB margin, so a margin of 7 dB will be assigned to the FSO UAV to satellite link. [14]

In order to attain a 7 dB margin on each of the uplink and downlink, the received power on both the uplink and downlink must be increased by roughly 8.5 dB to up -60.5 dBm. The path loss can be decreased by flying the UAV at a higher altitude, decreasing the range between the UAV and the satellite. To compensate for 8.5 dB, the path loss would be need to be reduced to 281.7 dB, or $1.48 \cdot 10^{28}$ W/W. The new altitude, d, is calculated to be

$$\begin{aligned} L_s &= 1.49 \cdot 10^{28} = \left(\frac{4\pi d}{\lambda}\right)^2 \\ d &= \sqrt{1.49 \cdot 10^{28}} \cdot \left(\frac{1550 \cdot 10^{-9}\ \mathrm{m}}{4\pi}\right) = 15001\ \mathrm{km} \end{aligned} \tag{4.18}$$

This is an extremely high altitude and greatly increases the path loss between the ship and the UAV. The pointing loss is relatively small, and even if it were eliminated altogether, it would not be enough to realize a 7 dB margin. The received power can be increased by using a larger EIRP. A different system than the Elliptica can be used, and as seen earlier, the antenna size can be changed to adjust the EIRP. In the RF case, the EIRP was decreased by reducing the antenna size, but here, we can increase the aperture to boost the EIRP, thereby satisfying our link margin constraint. The EIRP for the satellite and the UAV must each be increased by 8.5 dB to 125.5 dBm, or $3.55 \cdot 10^{12}$ mW.

$$\begin{aligned} \text{EIRP} &= P_t \cdot G_{t,FSO} = P_t \cdot \frac{4\pi^2 a^2}{\lambda^2} 0.81 \\ 3.55 \cdot 10^{12} \text{ mW} &= 15 \text{ mW} \cdot \frac{4\pi^2 \cdot \left(a^2 \text{ m}\right)}{\left(1550 \cdot 10^{-9} \text{ m}\right)^2} \cdot 0.81 \\ a &= 0.13 \text{ m} \end{aligned} \tag{4.19}$$

This aperture is about 10.5 in. in diameter, and would be much smaller than the RF antenna used on the UAV.

I. CHAPTER SUMMARY

Through analysis of the link budget, we were able to determine that an RF ship to UAV and FSO UAV to satellite link could be expected to perform with an uplink and downlink BER of $1 \cdot 10^{-6}$, or $2 \cdot 10^{-6}$ overall, at 2 Gbps. There was sufficient margin that the ship's antenna could be reduced to about one foot in diameter and still maintain the data rate and BER performance requirements.

The commercial FSO system available to the author, Terabeam's Elliptica 7421i is not suitable for the high data rate UAV to satellite link. The necessary optical link specified here has a transmit power of 15 mW, a wavelength of 1550 nm, a dark current of 1.5 nA, and a 10.5 in. obscuration free lens.

Next we will examine possible UAV candidates to mount the necessary communication systems. Factors to examine will include time on station, operating altitude, and cargo capacity, both in physical area and power availability. Operational concepts such as launching and recovering the UAV will also be addressed.

V. UAV SELECTION

In the ship-UAV-satellite link, the UAV is the crucial relay, providing the mechanism to route the ship's signal to the satellite and vice versa. Once the signal is received and demodulated in the UAV, it is assumed that the routing of information is possible through the use of high speed IP routers. The platform that will accommodate the communication and networking equipment is a critical design choice. Since the communications link will only be available as long as the UAV is operable, specifications of the UAV can directly affect the performance and utility of the link. Some of these specifications include the amount of time the UAV can stay aloft, the altitude at which it can operate, the payload that it can carry, available power to the payload, and options for launching and recovering the UAV.

A. REQUIREMENTS FOR A UAV RELAY

In order to make a sound choice for the type of UAV selected, the constraints should be identified. Not only will the UAV have to accommodate the size and power requirements for the communications equipment, but it must also remain airborne at an appropriate altitude for a substantial amount of time. Unlike a satellite that is put into orbit and remains for upwards of 10 years, the UAV, or system of UAVs, will have to be launched and recovered much more often. The type of UAV selected will determine how it is deployed. If the deployment method favors only a handful of operational units, the benefits of this architecture may not be realized.

1. Payload

The UAV must be able to carry and house the communication equipment. This includes the antennas, radios, routers, and racks for securing the equipment. Since we've modeled the UAV RF payload on the DSCS III satellite in the analysis section, we'll use some of those specifications for weight and power consumption here. The total weight of the DSCS III satellite is about 2580 lbs, including solar arrays, batteries, thrusters, and antennas that won't be used in this application. The power supply provides 1.2 kW and is supported by three 35 Amp-hour Ni/Cd batteries. Since the DSCS III has a main beam antenna EIRP of 40 dBW, we refer to the approximated antenna gain of 37.5 dB for the

45 in. main beam antenna from the previous chapter and calculate the required amount of transmit power to be $(P_t)_{dB} = (\text{EIRP})_{dB} - (G_t)_{dB} = 2.5\ dBW$, or 1.8 W. [28]

The proposed FSO system is very similar to the Terabeam Elliptica 7421i, but in order to successfully close the link at 2 Gbps and less than $1 \cdot 10^{-6}$ BER, it was necessary to increase the size of the aperture as discussed in chapter IV. The Elliptica's dimensions are approximately 11 x 12 x 14 in., with a weight of about 14 lbs. The power module is 3 x 5 x 10 in. and weighs 3 lbs. Increasing the aperture would certainly increase the size and weight of the transceiver, but not necessarily increase the power demands of the unit itself. Since the aperture needs to be increased by roughly 2.7 times the current 10 cm diameter, a conservative three-fold increase will be made to each of the dimensions as well as the weight. The final estimated size and weight of the FSO transceiver is 33 x 36 x 42 in. and 42 lbs. [30]

Tracking systems must be employed for the FSO system. The RF system should also use a tracking system in the event the UAV is not operating above the user, and also to track users within or nearby the strike group for ship-UAV-ship communications. Since the location of the UAV could give away the location of a unit, the ability for the link geometry to change makes the unit's location more ambiguous. The Elliptica transceiver has a beam steering mechanism built into the device, as shown in Figure 20.

Figure 20. Beamsteering Mirrors in the Terabeam Elliptica 7421i

The reason for this is to counteract the effects of building sway when the transceivers are mounted on tall buildings [35]. This tracking system is meant for two relatively immobile structures and is likely not adequate for a UAV mounted system.

When the RF signal reaches the UAV, it is demodulated and could either be converted to an optical signal and sent to the satellite or routed back through the RF antenna to another unit. The router should be able to switch at a high speed to prevent a bottleneck in the link. A candidate system, Cisco System's 12008 Series Router, is selected. It has a capacity of up to 40 Gbps bandwidth, and supports many different network interfaces. The dimensions of the router are 24.0 x 17.3 x 21.2 in, and its weight is 187 lbs. Typical power consumption is specified to be 1.62 kW. [36]

The total payload requirement is the sum of weight, space, and power needs of the RF and FSO equipment, the tracking system, and the networking hardware. To estimate the power and weight requirements of the payload, we will follow Lambert and Casey's postulated systems for an RF and FSO intersatellite link [20] and add the networking hardware. Both systems will use a gimbaled pointing system, with the RF system weighing 140 lbs and needing 150 W of power, and the FSO system weighing 106 lbs

and requiring 126 W [20]. The total weight and power requirements are 396 lbs and 1.3 kW. A summary of the payload requirements is shown in Table 4.

	Weight	**Power Required**
RF Components	140 lbs	150 W
FSO Components	106 lbs	126 W
Router	187 lbs	1.62 kW
Total	433 lbs	1.9 kW

Table 4. UAV Payload weight and power requirements

2. Loiter Time

The link is only available when the UAV is aloft. In order to provide continuous access, a method of relieving UAVs when they run out of fuel or power must be employed. If the UAVs have short loiter times, the operational cycle will be small, meaning more turnovers will need to take place. Accident rates and maintenance costs are more influenced by the number of flights a UAV makes rather than the number of flight hours [37]. So between launching and recovering more times or increasing the endurance of the UAV, extending the loiter time is favored to reduce the added complexity of maintaining the link.

3. Altitude

The UAV should operate at an altitude where it is above the highest clouds and in the portion of the atmosphere that has few particles that could cause scattering and absorption. Figure 21 shows where different cloud types reside in layers of the atmosphere.

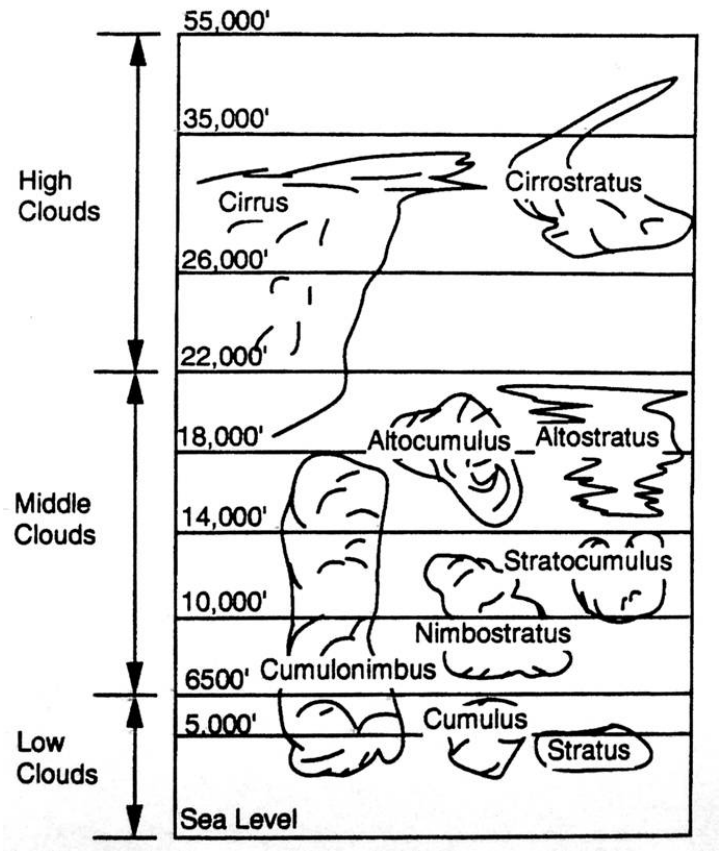

Figure 21. Cloud Types and Their Position in the Atmosphere (From [20])

In the previous chapter, the altitude was set at 65,000 ft, or 19.8 km. This puts the UAV at a level comfortably above the highest clouds.

4. Deployability

Since naval units are expected to operate far from any land-based runways, the UAV should not be restricted to such a fixed infrastructure. If a runway is needed, the UAV's range and time on station should be sufficient so that a ship can take advantage of the link without cycling through many UAVs. If the UAV can be deployed from the ship itself, the number of flights may be reduced since there will be less distance for the UAV to transit to the operating area. However, while it may be relatively simple for an aircraft carrier to launch and recover UAVs, it may prove more difficult for a destroyer, or a submarine.

B. TYPES OF UAVS

There are several different designs and purposes for employing UAVs, but we will restrict our review to the high-altitude, long-endurance (HALE) platforms. In this category, there are fixed wing, vertical take off and landing (VTOL), and lighter than air design schemes. Within these schemes, examples of UAVs are presented with their system specifications to determine the most suitable candidate.

1. Fixed Wing

Fixed wing UAVs are currently in service supporting Operation Enduring Freedom and Operation Iraqi Freedom in surveillance as well as attack roles. Their proven utility and flexibility have made them an important asset, used by all the U.S. military services as well as those in the intelligence community. [38]

a. Predator B

The Predator B is an enlarged HALE version of General Atomic's medium-altitude RQ-1 Predator. The Predator B has three variants, the Altair, built primarily for NASA, the Mariner, a proposed candidate for the U.S. Navy's Broad Area Maritime Surveillance program, and the Hunter-Killer, a U.S. Air Force version capable of carrying up to 14 Hellfire missiles. The Predator B, shown in Figure 22 as the Mariner, retains much of the same appearance as the original Predator except for the tail configuration and added fuel tank.

Figure 22. General Atomics' Predator B, Altair Variant Flying as the Mariner (From [39])

Some of the internals of the Mariner variant are shown in Figure 23. Of particular note are the satellite antenna, the maritime surveillance radar in the pod on the Mariner's belly, and the under-nose targeting system and radar. [39]

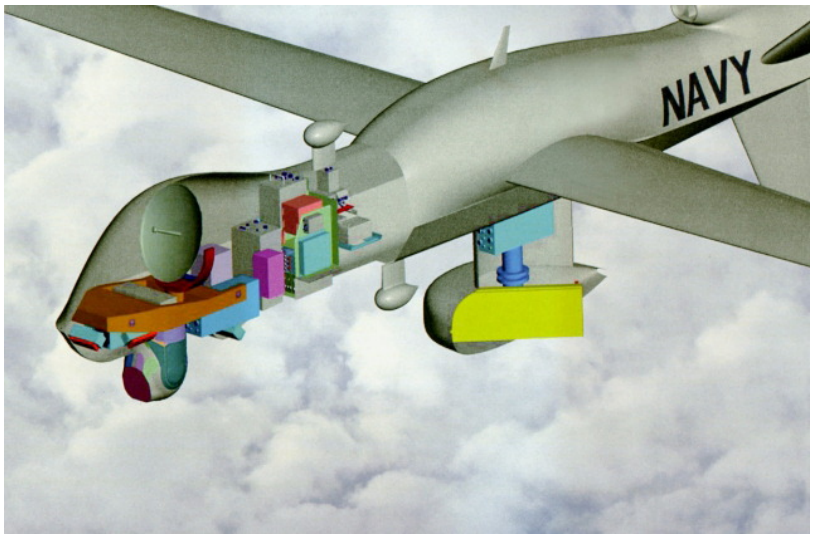

Figure 23. Internal detail of Mariner BAMS proposal (From [39])

The specifications of the Predator B, Mariner variant are summarized in Table 5.

Wing span:	26.21 m (86 ft 0.0 in)
Length overall:	11.03 m (36 ft 2.4 in)
Fuselage max width:	1.13 m (3 ft 8.4 in)
Height overall:	3.59 m (11 ft 9.5 in)
Wheelbase:	3.09 m (10 ft 1.5 in)
Propeller diameter:	2.79 m (9 ft 2.0 in)
Payload bay volume (total):	1.30 m^3 (46.0 cu ft)
Max fuel weight:	2,722 kg (6,000 lb)
Max payload (internal):	522 kg (1,150 lb)
Max payload (external):	907 kg (2,000 lb)
Max level speed:	240 kt (444 km/h; 276 mph)
Max operating altitude:	15,850 m (52,000 ft)
Endurance:	>49 h

Table 5. Specifications for Predator B, Mariner Variant (After [39])

With 10 kW of power available and ample payload room for the networking hardware, the Predator B may be a suitable choice. As shown in Figure 23, the RF dish antenna is on top of the aircraft. In the ship-UAV-satellite architecture, the RF dish antenna would need to be pointed downward or the UAV would have to fly inverted. With a maximum fuselage width of 1.13 meters, the RF antenna size may have to be reduced, since the previous link budget used the DSCS III antenna diameter of 1.1 m. An external pod, similar to the targeting turret in the front of the Mariner, should be attached to the top of the UAV to house the FSO transceiver. Unfortunately, the maximum operating altitude is beneath our threshold. Changes would need to be made to the laser link in terms of antenna size or power provided, but the atmospheric absorption and scattering due to clouds should be fairly minimal as shown previously in Figure 21. The additional free space loss is only about 2 dB, easily overcome by modifying the FSO transceiver.[39]

Unfortunately, this aircraft is quite large and would need to be launched and recovered from a runway [39]. It may be possible to install arresting gear and to

fortify the landing gear for aircraft carrier operations, but a small ship would not be able to launch this particular UAV.

b. Global Hawk

The RQ-4A Global Hawk, like the Predator B, is another large fixed wing UAV capable of high altitude operations for extended periods of time. Figure 24 shows the mission concept for the Global Hawk.

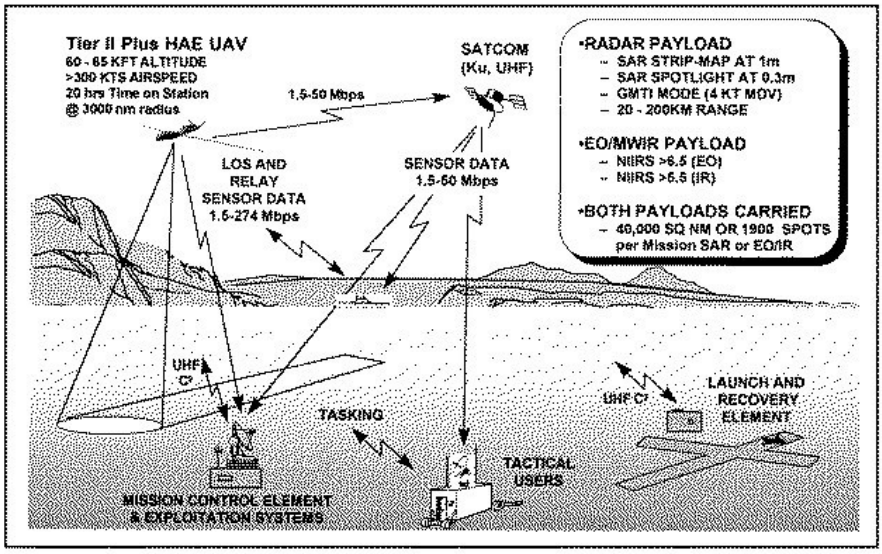

Figure 24. Global Hawk Mission Concept (From [40])

The Global Hawk is used in a surveillance and reconnaissance role, as opposed to the Predator which has the ability to carry and fire weapons. Like the Predator, the Global Hawk has the ability to communicate via satellite with its up-facing antenna shown in Figure 25.

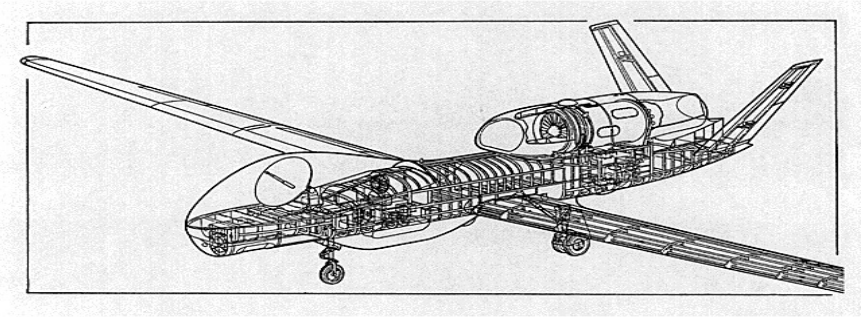

Figure 25. Global Hawk Cutaway (From [40])

Because of the antenna orientation, modifications would again need to be made so that Global Hawk could communicate with units below. A turret should be added to house the FSO transceiver and tracking apparatus as well. The specifications for the Global Hawk are shown in Table 6.

Wing span:	35.41 m (116 ft 2.0 in)
Length overall:	13.51 m (44 ft 4.0 in)
Fuselage max width:	1.45 m (4 ft 9.0 in)
Height overall:	4.39 m (14 ft 5.0 in)
Weight empty:	4,173 kg (9,200 lb)
Max fuel weight:	6,577 kg (14,500 lb)
Max payload:	907 kg (2,000 lb)
Loiter speed:	343 kt (635 km/h; 395 mph)
Loiter altitude:	15,240-19,810 m (50,000-65,000 ft)
Service ceiling:	>19,810 m (65,000 ft)
Max endurance:	35 h

Table 6. Specifications for Global Hawk, RQ-4A (After [40])

The available 25 kW of power, large payload capacity, and high altitude make the Global Hawk an attractive possibility as the UAV relay. [40]

As with the Predator B, this UAV is quite large and heavy. Figure 26 lends perspective on the size of this aircraft.

Figure 26. Global Hawk at Beale Air Force Base (From [40])

Even an aircraft carrier may find it difficult to launch and recover the Global Hawk with its large wingspan, making a base with a runway essential.

c. Helios

The Helios is an experimental solar powered UAV capable of tremendous endurance. Designed by AeroVironment Inc. for a NASA program at Dryden Flight Research Center, the Helios has wings covered with solar panels and is propelled by eight two-bladed propellers. The solar cells generate 42 kW of power and fuel cells charge during the day for night flights. This is a large advantage when fuel costs are compared. The Helios prototype is shown in Figure 27.

Figure 27. Helios Prototype in July 2001 (From [41])

The specifications for the Helios are shown in Table 7. [41]

Wing span:	75.29 m (247 ft 0.0 in)
Length overall:	3.66 m (12 ft 0.0 in)
Weight empty:	Approx 726 kg (1,600 lb)
Max payload:	100 kg (220 lb)
Max level speed:	28 kt (51.5 km/h; 32 mph)
Altitude:	15,240-21,340 m (50,000-70,000 ft)
Endurance:	6 months

Table 7. Specifications for Helios (After [41])

Lacking any satellite communication equipment, the necessary payload weight for the RF and the FSO systems will exceed the maximum payload of the Helios. The largest of the fixed winged aircraft discussed here, ship deployment is out of the question. However, because of its long endurance, a network of aloft UAVs could be employed. The UAVs could loiter in their locations even if there were no users nearby.

Then, if a unit came into range, the Helios would be ready to facilitate high speed communications. An added benefit of this architecture is that the position of a unit is not given away since the UAV will be aloft even when no users are communicating. Unfortunately, many UAVs would be needed to provide global coverage. A UAV, or a network of UAVs could move with the strike group, reducing the number of UAVs and handoffs required, but providing an adversary with a possible means of locating deployed units.

2. VTOL

UAVs that have the ability to take off and land without runways can be employed on small ships easier than the previously discussed larger fixed wing aircraft. Unfortunately, there are relatively few HALE UAVs that have this capability. One exception under development is the A-160 Hummingbird. The Hummingbird is being developed under DARPA's Advanced Technology Demonstration project. A computer graphic of the Hummingbird is shown in Figure 28.

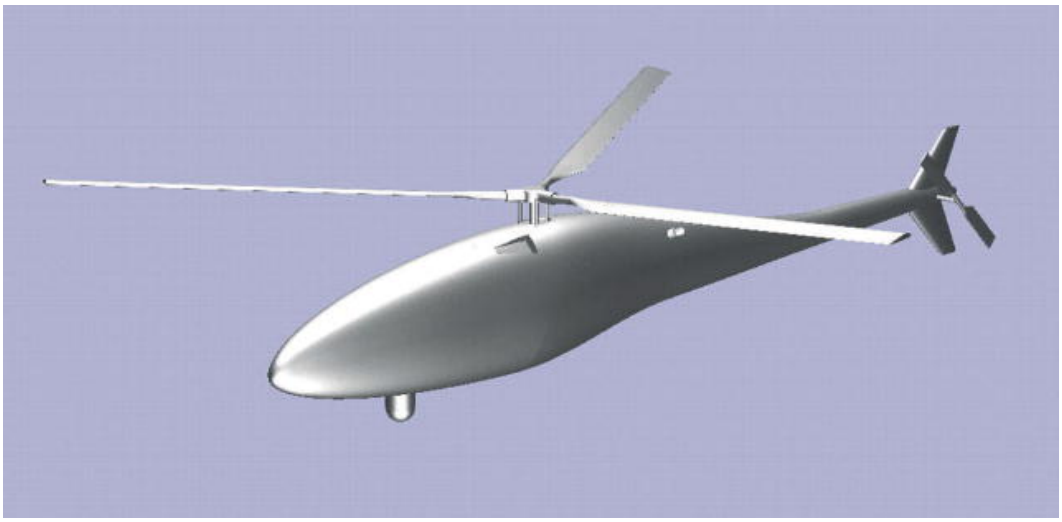

Figure 28. A-160 Hummingbird Illustration (From [42])

The specifications for the Hummingbird are summarized in Table 8. [42]

Main rotor diameter	9.75 m (33 ft)
Fuselage length	10.7 m (35 ft)
Payload bay volume in nose:	3.1 m^3 (110 cu ft)
Max payload	136 kg (300 lb)
Max level speed	Approx 140 kt (259 km/h; 161 mph)
Max operating altitude	9,145 m (30,000 ft)
Hovering ceiling OGE	4,570 m (15,000 ft)
Range	2,500 nm (4,630 km; 2,877 miles)
Endurance	30-40 h

Table 8. Specifications for A-160 Hummingbird (From [42])

Although the ability for the Hummingbird to hover in one place may make the ship-board tracking system simpler, and the endurance is very good, mounting the antennas may be somewhat difficult. The overhead rotors could cause adverse affects to the FSO signal, unless the transceiver can be mounted above or to the side of the rotors. The diameter of the main rotor is large, but smaller than the rotors of some helicopters that deploy from U.S. Navy Destroyers [43]. The altitude is also well below the desired threshold.

3. Lighter than Air

The last group of HALE UAVs under consideration is the lighter than air (LTA) variety. This category involves platforms that are essentially balloons or blimps.

a. 420K Aerostat

Lockheed Martin's 420K is a tethered aerostat used for radar surveillance. It has the ability to detect, identify and track targets as well as relay data. Unfortunately, because it is tethered, its altitude and maneuverability is limited by its connection to the ground. The 420K could be deployed from a ship, but aircraft would need to avoid the tether and harsh winds could prevent deployment. Table 9 shows the specifications, and Figure 29 shows a picture of the 420K at a mooring station.

Length	63.55 m (208 ft 6.0 in)
Max diameter	21.18 m (69 ft 6.0 in)
Radome diameter:	12.19 m (40 ft 0.0 in)
Antenna: Width x Height	8.84 m (29.0 ft) x 5.18 m (17.0 ft)
Payload capability:	952.5 kg (2,100 lb)
Operating altitude	4,575 m (15,000 ft)
Radar detection range	200 n miles (370 km; 230 miles)
Endurance	5-7 days

Table 9. Specifications for Lockheed Martin 420K (After [44])

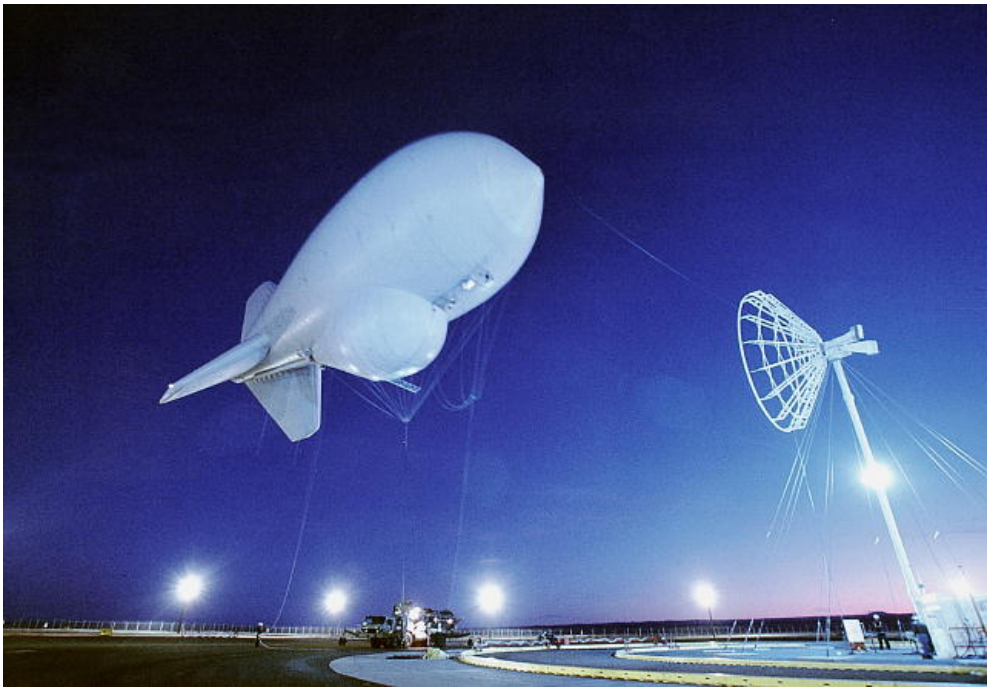

Figure 29. Lockheed Martin 420K Aerostat (From [44])

This balloon will not satisfy the needs for the UAV relay. Although the endurance and payload are adequate, the limited altitude and the requirement for a tether are undesirable.

b. Aerosphere Airship

TechSphere Systems International's Aerosphere is a spherical shaped, high altitude LTA airship. The Aerosphere has its own station keeping system and does not require tethers. The airship is designed to act in a surveillance role as well as a

communications relay. Figure 30 shows an illustration of the Aerosphere and its possible coverage area. [45]

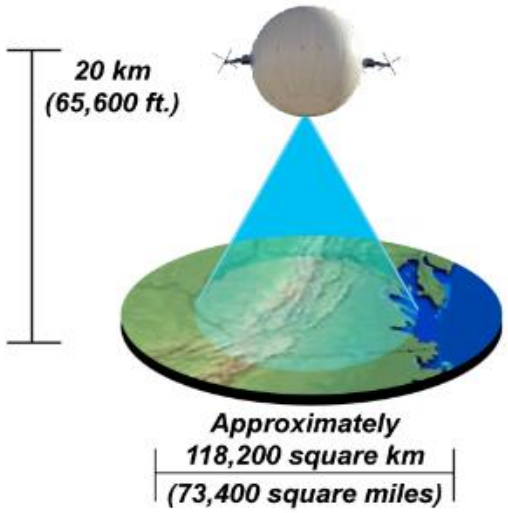

Figure 30. Footprint of TechSphere's Aerosphere (From [46])

Under development and testing, the Aerosphere is projected to have a very long endurance time and also be able to lift a relatively heavy payload. Table 10 shows the specifications.

Max diameter	300 ft
Engines	3
Operating altitude	20,000 m (about 65,000 ft)
Endurance	6 months, up to 1 year

Table 10. Specifications for Techsphere's Aerosphere (After [47])

Power and payload capacity and specifications are not available; however, the Naval Air Systems Command has conducted testing with the smaller 62 ft diameter Aerosphere that has a 22,000 ft ceiling. The payload of this craft is about 1000 lbs [47]. The smaller Aerosphere only has a two day endurance. [48]

If the power and payload available are adequate, the Aerosphere may be an excellent choice. Its configuration as a wireless relay shown in Figure 30 is well suited for the RF portion of the ship-UAV-satellite relay. Again, a FSO transceiver and tracking device will need to be attached. Although its diameter is most likely too large for deployment by a ship, the altitude and extremely long loiter time make the Aerosphere an attractive pre-positioned communications relay.

C. CHAPTER SUMMARY

Several options and platforms for the UAV relay were presented. Since none of them have an overhead FSO transceiver, all of the UAVs would need to be retrofitted with such a device. The fixed wing HALE UAVs require a runway nearby, but their specifications indicate feasibility, especially with the long endurance of the Helios, making launching and recovery less frequent and keeping fuel costs low. If the Aerosphere can be fitted with the necessary communications payload, its altitude and long loiter time make it an ideal candidate.

Next, experimentation with a commercial FSO system and IEEE 802.11b links is discussed. Portable 802.11b links will represent the RF portion of the ship-UAV-satellite communications architecture. The effect of having such a large bandwidth link in concert with the RF links in a variety of configurations will be shown.

THIS PAGE INTENTIONALLY LEFT BLANK

VI. EXPERIMENT

Similar to the proposed ship-UAV-satellite link, a composite RF and FSO network was set up on a much smaller scale. The goal of the experiment was to determine if the addition of a fast FSO link would affect the overall data transfer when the user has a slower RF link. If the FSO link or the routing from the RF to the FSO link introduces packet errors in the transfer, transmission control protocol (TCP) will cause a retransmission of those packets [49] and slow down the overall transfer.

A. SET UP

The experiment took place on the roof of Spanagel Hall at the Naval Postgraduate School in Monterey, CA on the morning of August 24, 2005. The weather conditions at the nearby Monterey Airport are summarized in Table 11.

Time	1000	1100	1200
Wind (direction and mph)	W 5	SW 6	SW 5
Visibility (miles)	5	5	8
Weather	Mist	Mist	
Sky Conditions	Overcast	Overcast	Overcast
Ceiling (feet)	300	300	500
Temperature (°F)	55	55	55
Dewpoint (°F)	53	53	52
Relative Humidity	93	93	89
Barometric Pressure (inches)	29.82	29.82	29.82

Table 11. Weather conditions at the Monterey Airport on August 24, 2005 (After [50])

The ship to UAV portion was modeled with 2 Hewlett Packard h6315 iPAQ Pocket PCs and a Dell Inspiron 9300 (i9300) laptop as shown in Figure 31.

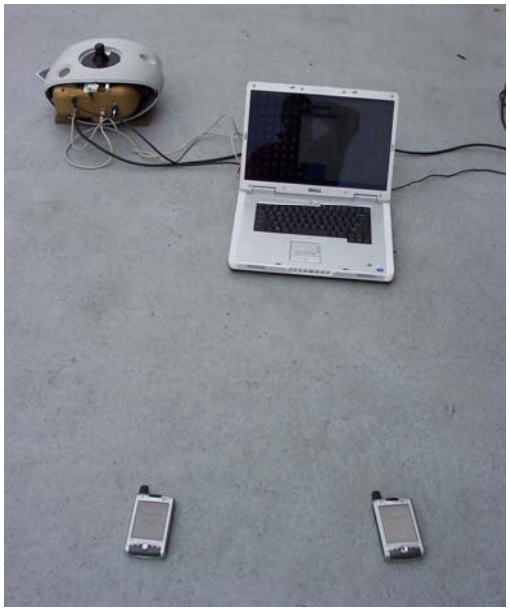

Figure 31. Hewlett Packard h6315 iPAQs, Dell i9300 and Terabeam Elliptica 7421i.

The iPAQs and the i9300 laptop were all enabled with IEEE 802.11b (Wi-Fi) radios that have a maximum data rate of 11 Mbps [51]. The UAV to satellite link was represented with the i9300 connected to a Dell Inspiron 5150 (i5150) laptop via a pair of Terabeam Elliptica 7421i FSO transceivers that have a maximum data rate of 100 Mbps [30]. The distance between the iPAQs was about 2 ft, while the distance between the iPAQs and the i9300 was roughly 3 ft. The separation of the two FSO transceivers was about 300 ft. Line of sight was maintained for all links. Figure 32 shows the setup from the RF link side, with the other Elliptica and the i5150 in the far background.

Figure 32. Experiment set up with RF link in the foreground

The experiment consisted of transferring a 1.36 MB data file from the iPAQs to the i5150 using Server Message Block (SMB) protocol and TCP. SMB is a protocol that allows communication and file sharing between computers [52], while TCP provides a reliable connection between them [49]. A packet analyzer, Ethereal, was installed on the i5150 and used to determine the amount of time it took for the file to transmit. In order to determine how the FSO link affected the transmission, Ethereal was also installed on the i9300 and the file transfer was repeated without the laser link. In a variety of configurations discussed next, the iPAQs used a Wi-Fi link to the i9300 and the i9300 relayed to i5150 across the FSO link. The i9300 and i5150 each connect to the "Data" port on the FSO transceivers by a Category-5 Ethernet cable as shown in Figure 33.

Figure 33. Elliptica 7421i Ethernet connection

B. NETWORK CONFIGURATION

In order to communicate to one another within the network, all the devices are provided with addresses, as shown in Table 12, and the layout of the entire network showing IP addresses is illustrated in Figure 34.

Device	**Wi-Fi port IP Address**	**Wi-Fi port MAC Address**	**Ethernet port IP Address**	**Ethernet port MAC Address**
i9300	192.168.0.1	00:11:f5:22:39:27	192.168.0.100	00:11:43:76:25:89
i5150	N/A	N/A	192.168.0.101	00:0f:1f:23:16:fa
iPAQ h6315	192.168.0.10	00:0b:6b:54:96:cf	N/A	N/A
iPAQ h6315	192.168.0.15	00:0b:6b:54:7b:15	N/A	N/A
Elliptica 7421i	N/A	N/A	192.168.0.200	00:03:55:01:00:7b
Elliptica 7421i	N/A	N/A	192.168.0.201	00:03:55:01:00:4a

Table 12. IP and Hardware address for devices used

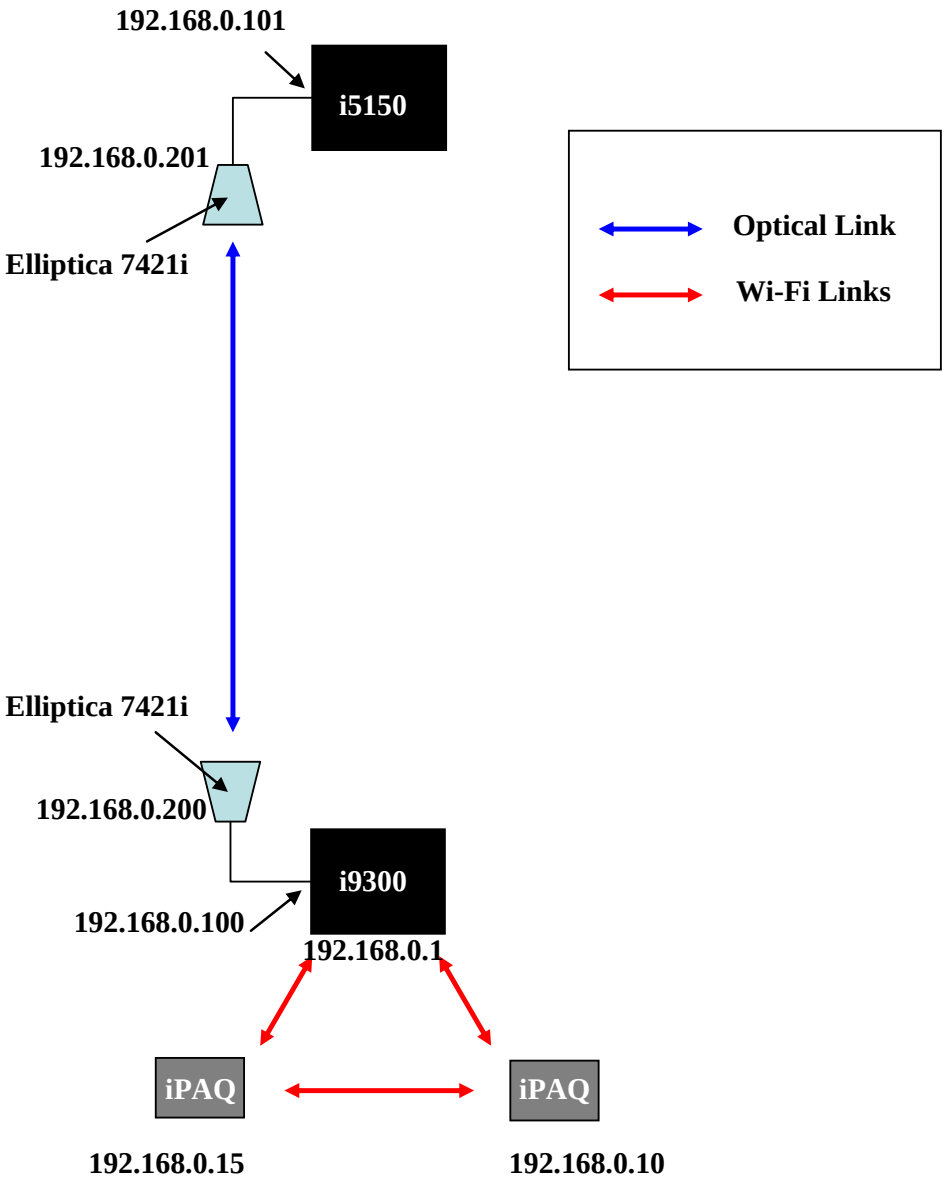

Figure 34. Diagram of entire network showing IP addresses

The connections between the i9300 and i5150 laptops to the Elliptica transceivers are Category-5 Ethernet cables. Only the i9300 requires both a Wi-Fi and Ethernet address, since it acts as a router between the RF and the FSO links.

There are several configurations possible in the network. First, the RF network was established so that the iPAQs communicated directly to the i9300. This first configuration did not support multi-hop, or using one of the Pocket PC's as a relay. In

the ship-UAV link, there could be a situation where a ship was not in range of the UAV, but was in range of another ship that did have connectivity. The scenario in Figure 35 illustrates this case where the USS Essex had the ability to communicate with the USS Chancellorsville via the USS Fort McHenry and the airborne P-3 during the U.S. Navy's Trident Warrior 2003 exercise [53]. To simulate this situation, the routing tables of one of the iPAQs and the i9300 were changed. Even though both of the Pocket PC's were in range of the i9300, one of the iPAQs was forced to transmit to the other iPAQ, and the i9300 was forced use this same relay. Before the transfer took place, the traceroute network utility was used to verify the paths were correctly set in place. Finally, this multi-hop network was tested when both iPAQs transmitted at the same time.

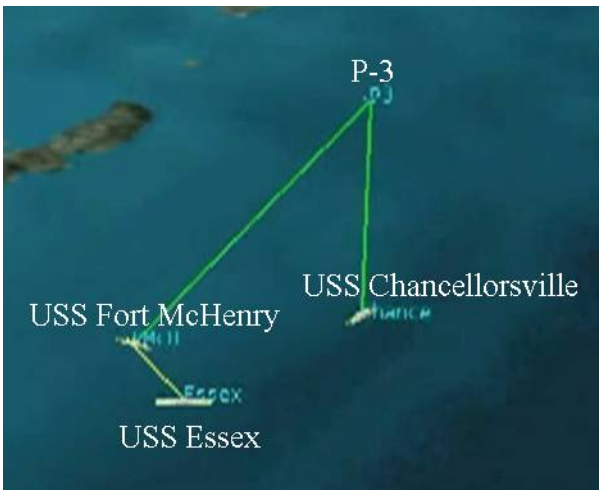

Figure 35. USS Essex communicating to USS Chancellorsville in Trident Warrior 03 (After [53])

The network and data transfer configurations are shown in Figures 36 through 40. In Figures 36 and 37, one iPAQ communicates while the other does not. In Figure 38, both iPAQs communicate directly with the i9300 simultaneously. In Figure 39, one iPAQ communicates and uses the other as a relay. In Figure 40, both iPAQs transmit the data file, and one of them is used as a relay.

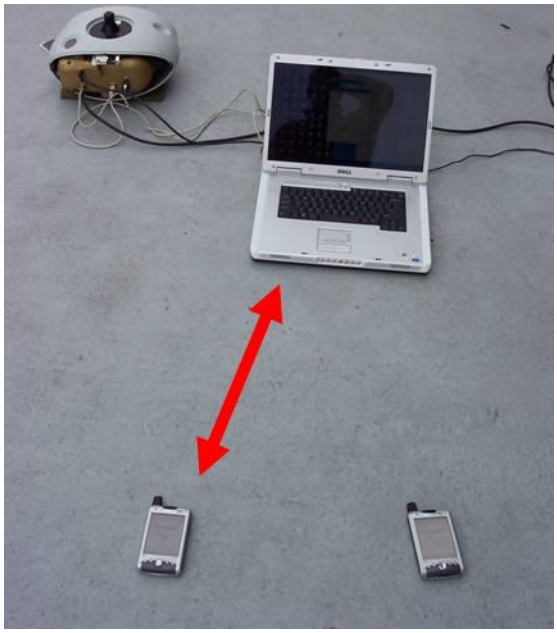

Figure 36. iPAQ 192.168.0.15 transmits to i9300

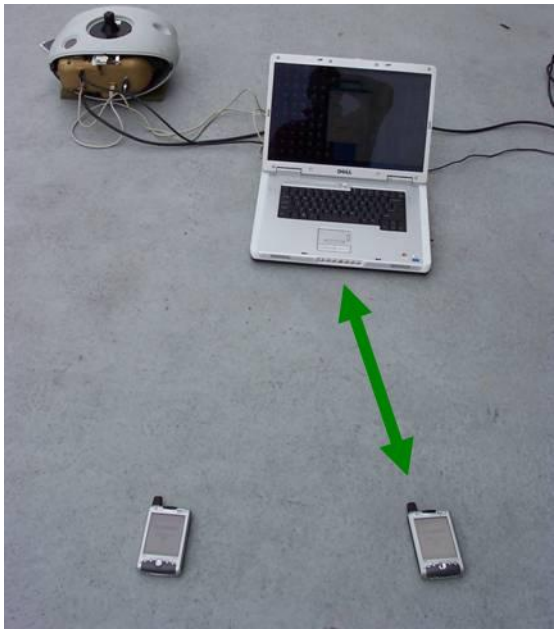

Figure 37. iPAQ 192.168.0.10 transmits to i9300

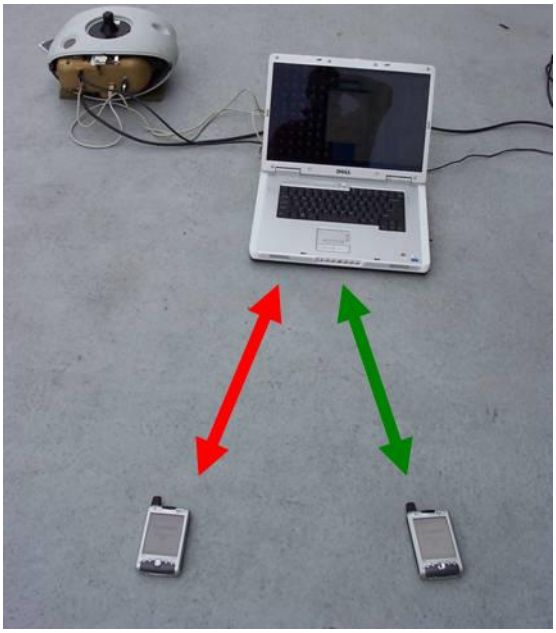

Figure 38. Both iPAQs transmit to i9300

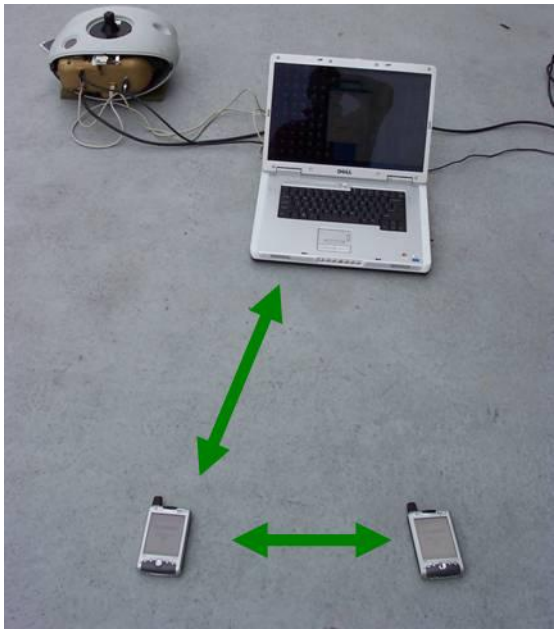

Figure 39. iPAQ 192.168.0.10 transmits to i9300, using 192.168.0.15 as a relay

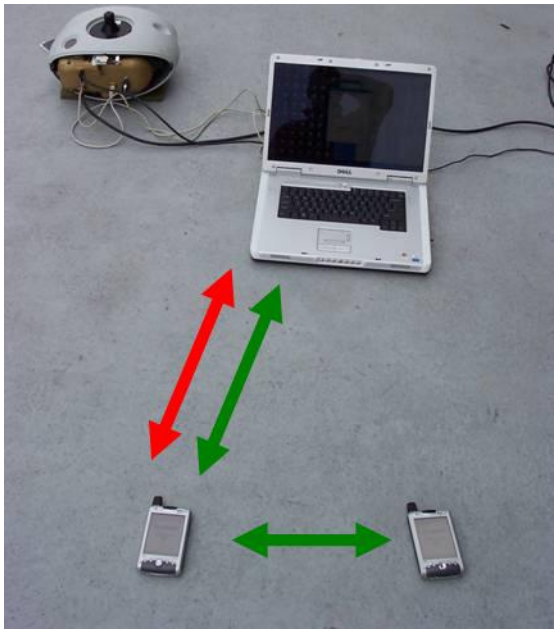

Figure 40. iPAQ 192.168.0.10 transmits to i9300, using 192.168.0.15 as a relay, while 192.168.0.10 also transmits

Since the iPAQs are sending the file to the i5150, the i9300 acts as a router. The i9300 sends the file to the Elliptica transceiver, transferring the file over the optical link, and reaches the i5150. After completing all file transfers for the configurations shown in Figures 36 through 40, the transfers were repeated, but sent to the i9300 instead of the i5150, so that the Wi-Fi link performance could be analyzed without the additional routing and transmission over the FSO link.

Within Ethereal, the packets were analyzed starting from the SMB "Open AndX Request" command and stopping at the 60 byte TCP packet acknowledging the SMB "Find Close2 Response" command. The "Open AndX Request" was sent when the iPAQ initiated transfer of the file to the i5150. The i5150 looked for the file in the specified directory, and when it was not found, the i5150 created a file of the same name and allowed the transfer to begin. Then, SMB "Write" packets allowed the incoming data to be put it into the created file. Finally, the file was closed with the "Find Close2 Response" command after verification that the data in the file had successfully been transferred and the file information had been set. File information consists of parameters about the file such as when the file was created, when it was last accessed, and file

attributes such as hidden, encrypted, or read only. A TCP/IP packet acknowledged the closing of the file and no more communication took place between the iPAQ and the i5150. By restricting the packet capture to this range, any packets sent before the "Open AndX Request" or after the final TCP packet were not involved with the file transfer did not interfere with the analysis.

C. RESULTS

The results of the data transfers over all the previously discussed network configurations are shown in the following figures, produced by Ethereal. Each figure consists of a summary of the transfer and a graph showing the data rate vs. the time it took to send the file. Within the summary, a filter was used to show the number of TCP retransmissions. Since TCP is a reliable transport layer protocol, if a packet is sent with an error, TCP requires the data to be retransmitted until it arrives without error [49]. So for every TCP retransmission there is at least one error in one packet. The column named "Captured" shows the entire transfer, while "Displayed" shows only the retransmitted packets. The need to retransmit packets is one reason for different amounts of packets being captured from one transfer to the next.

Figure 41 shows the summary and the data rate when only iPAQ 192.168.0.15 transmits to the i5150. For comparison, Figure 42 shows the summary and data rate of this configuration when the file is sent to the i9300 and the FSO link is not used.

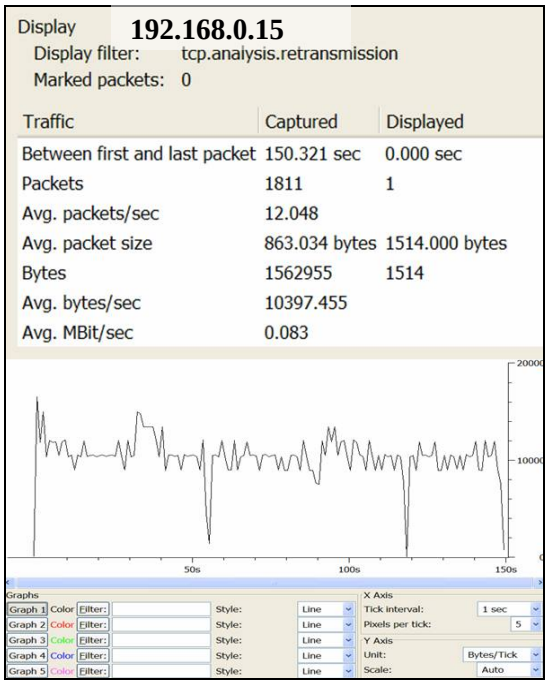

Figure 41. iPAQ 192.168.0.15 sends to i5150

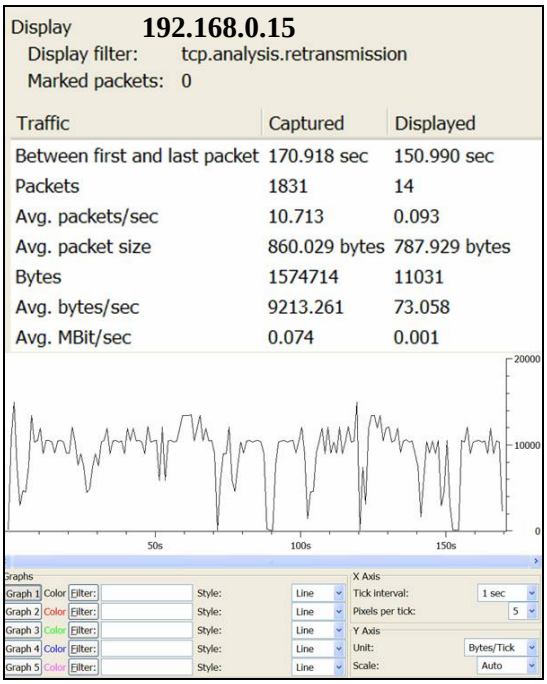

Figure 42. iPAQ 192.168.0.15 sends to i9300

It took 150.3 s for the iPAQ to transfer the file to i5150, and 170.9 s to the i9300. The longer amount of time to transmit the same file was due in part to the higher number of packet retransmissions when transferring to the i9300. In Figure 42, the average data rate for packet retransmission was very low compared to the overall average. This low bit rate delayed the data transfer.

Figures 43 and 44 show the file transfer by iPAQ 192.168.0.10 to i5150 and i9300 respectively. Again the transfer without the additional routing and the FSO link took more time. In this instance, the number of retransmissions was higher across the composite RF and FSO link. However, Figure 44 shows that for the transfer to the i9300, the data rate for packets needing retransmission was still lower, and that the average packet that had to be retransmitted was larger, leading to a higher overall transfer time.

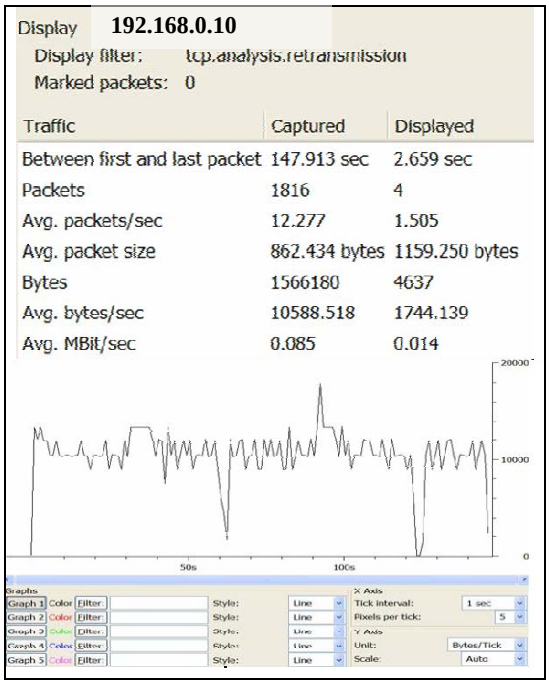

Figure 43. iPAQ 192.168.0.10 sends to i5150

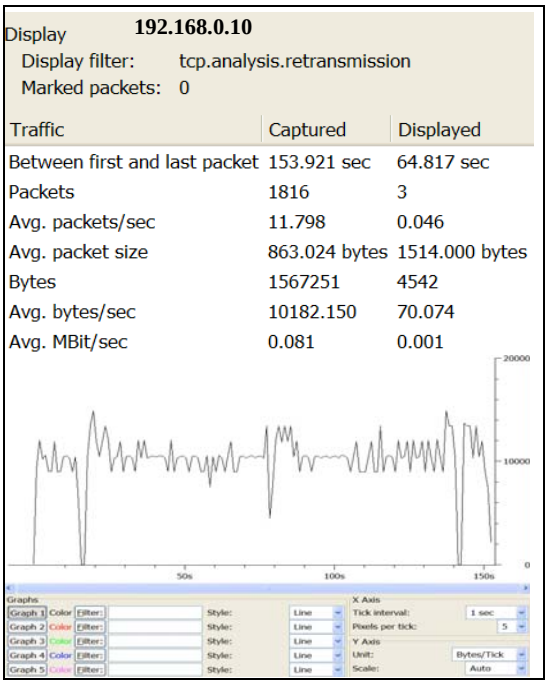

Figure 44. iPAQ 192.168.0.10 sends to i9300

Figure 45 shows the data transfer from both iPAQs to the i5150 at the same time. The summary on the left shows the retransmissions for 192.168.0.15 and the summary on the right shows the retransmissions for 192.168.0.10. The graph below the summaries shows the data rate of the transfers. The black line is represents 192.168.0.15's data rate, while the red indicates the data rate for 192.168.0.10. The blue line is the sum of their data rates over the transfer time. A comparison of the blue line in Figure 45 to the data rate graphs in Figures 41 and 43 shows similar results. This may indicate a maximum data rate for the link.

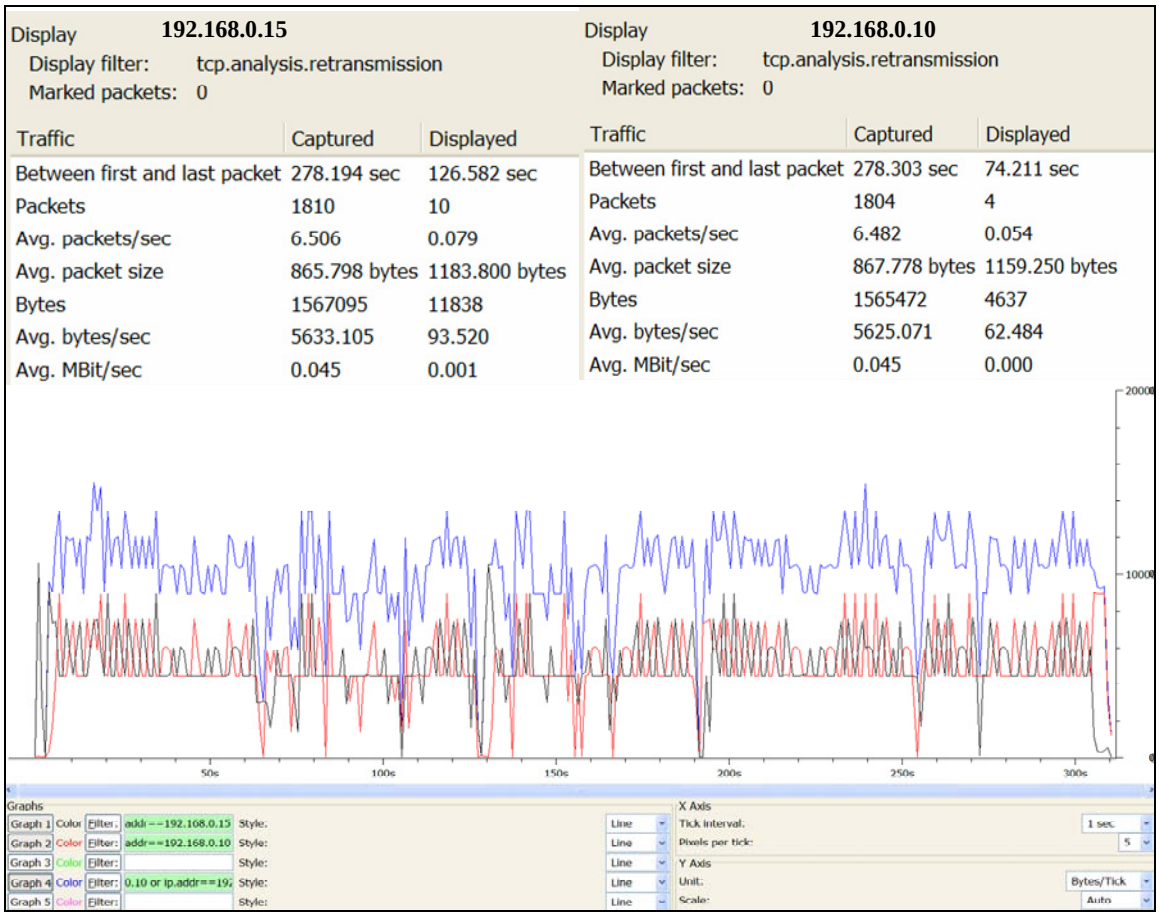

Figure 45. Both iPAQs transmit to the i5150 at the same time

Figure 46 shows the summary of the data being transferred when both iPAQs transmit to the i5150 at the same time. By looking at the blue line representing the total data rate in Figure 45 and the summary in Figure 46, it appears that the data rate for the link is limited and the iPAQs share the link equally, since the individual iPAQs each have an average data rate of roughly half the total data rate.

Display **192.168.0.15 and 192.168.0.10**
Display filter: (ip.addr==192.168.0.10 or ip.addr==192.168.0.15) and tcp.analysis.retransmission
Marked packets: 0

Traffic	Captured	Displayed
Between first and last packet	281.665 sec	200.488 sec
Packets	3614	14
Avg. packets/sec	12.831	0.070
Avg. packet size	866.787 bytes	1176.786 bytes
Bytes	3132567	16475
Avg. bytes/sec	11121.594	82.174
Avg. MBit/sec	0.089	0.001

Figure 46. Total summary of both iPAQs transmitting to i5150 at the same time

Figure 47 shows the results when both iPAQs transmit to the i9300 simultaneously. As in the case where they both send their files to the i5150, they appear to share the available link data rate equally.

Display **192.168.0.15**
Display filter: tcp.analysis.retransmission
Marked packets: 0

Traffic	Captured	Displayed
Between first and last packet	310.793 sec	269.651 sec
Packets	1841	15
Avg. packets/sec	5.924	0.056
Avg. packet size	860.845 bytes	930.933 bytes
Bytes	1584815	13964
Avg. bytes/sec	5099.268	51.785
Avg. MBit/sec	0.041	0.000

Display **192.168.0.10**
Display filter: tcp.analysis.retransmission
Marked packets: 0

Traffic	Captured	Displayed
Between first and last packet	309.794 sec	91.439 sec
Packets	1801	7
Avg. packets/sec	5.814	0.077
Avg. packet size	870.896 bytes	670.000 bytes
Bytes	1568483	4690
Avg. bytes/sec	5062.982	51.291
Avg. MBit/sec	0.041	0.000

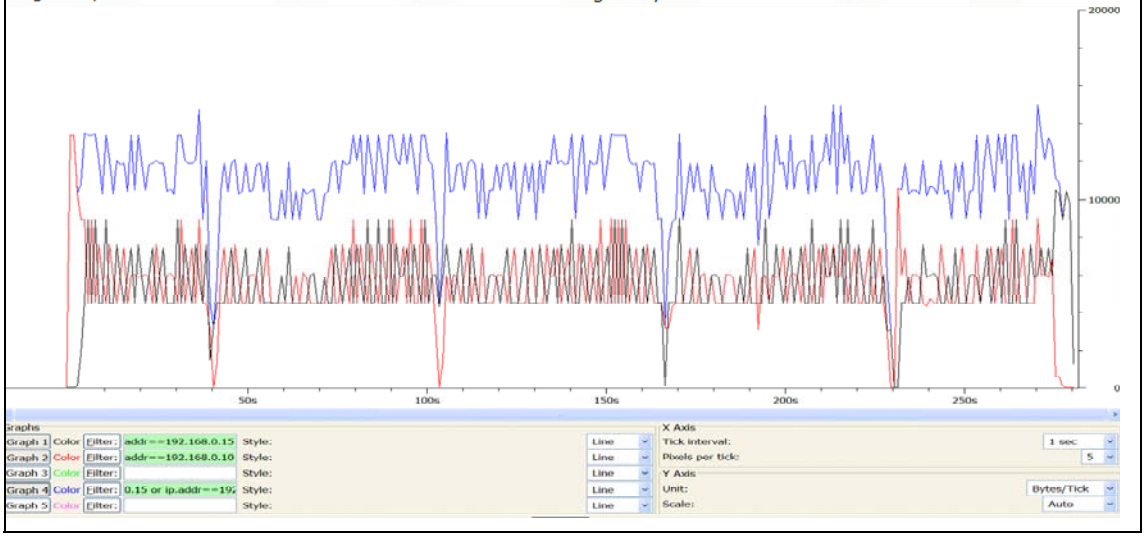

Figure 47. Both iPAQs transmit to i9300 at the same time

The time required to transfer the file and the average data rate attained by each iPAQ, as well as the overall data transfer, shown in Figure 48, suggest that the link is not limited by the FSO portion of the network. The Wi-Fi link or the SMB protocol may be responsible for limiting the data rate. If the FSO portion of the network were limiting the maximum data rate, the time needed to send the file to the i9300 would be less than the time needed to send the file to the i5150, but this is not the case.

Display **192.168.0.15 and 192.168.0.10**
Display filter: (ip.addr==192.168.0.10 or ip.addr==192.168.0.15) and tcp.analysis.retransmission
Marked packets: 0

Traffic	Captured	Displayed
Between first and last packet	311.781 sec	269.651 sec
Packets	3644	22
Avg. packets/sec	11.688	0.082
Avg. packet size	865.363 bytes	847.909 bytes
Bytes	3153382	18654
Avg. bytes/sec	10114.081	69.178
Avg. MBit/sec	0.081	0.001

Figure 48. Total summary of both iPAQs transmitting to i9300 at the same time

In the next configuration, 192.168.0.10 is the only iPAQ that transmits, but it uses 192.168.0.15 as a relay. The iPAQ that becomes the relay does not send its own data, but passes along packets from sender to receiver. Figure 49 shows the transfer to the i5150, while Figure 50 shows the transfer to the i9300.

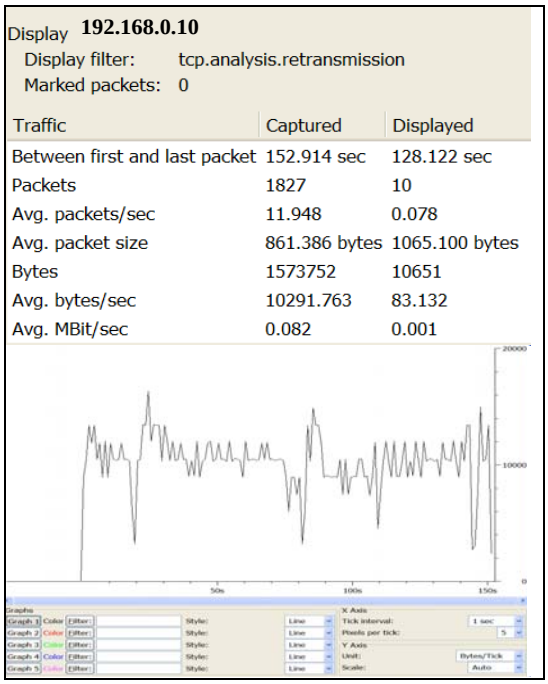

Figure 49. iPAQ 192.168.0.10 sends to i5150, using 192.168.0.15 as a relay, while 192.168.0.15 does not send

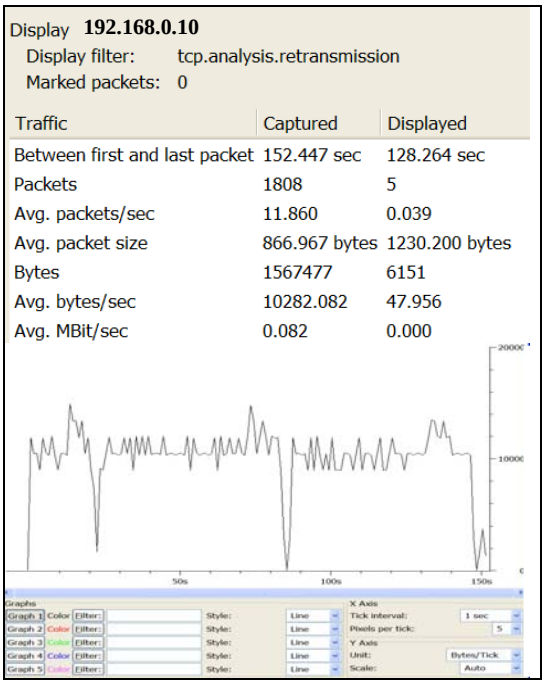

Figure 50. iPAQ 192.168.0.10 sends to i9300, using 192.168.0.15 as a relay, while 192.168.0.15 does not send

The results from Figures 49 and 50 show that the additional hop does not significantly change the time it takes for the iPAQ to transfer the file, nor does it produce a large increase of packet retransmissions. The fact that the file transfer does not take longer, despite two iPAQs effectively competing for access to the wireless medium is an interesting result. The set-up of the relay was verified with traceroute from the originating iPAQ, as well as the i9300 to confirm that 192.168.0.15 was being used as a relay and not being bypassed. Aside from a human error in configuring the routing tables, another possible reason for the result is that the links between the iPAQs and the link between the iPAQ and the i9300 could be on non-interfering Wi-Fi channels. This would enable both iPAQs to transmit or receive simultaneously, but only if the relay had more than one Wi-Fi card. Unfortunately, this is not the case. The author believes that the reason for this result is due to bridging the Ethernet and Wi-Fi connections. The Wi-Fi network card on the i9300 does support promiscuous mode. As a result, the data rate capacity indicated on the Windows XP Taskbar drops from 11 Mbps to 1 Mbps. The

actual throughput is less. Between the iPAQs, the data rate stays high, but between the relay iPAQ and the i9300, the throughput drops. Effectively, the delay is between 192.168.0.15 and i9300, and the additional hop slows transmission by an insignificant amount. Microsoft describes problems with non-promiscuous mode Wi-Fi cards in [54].

The last test also uses this multi-hop configuration, but instead of just one iPAQ transmitting, both devices send the file to the i5150. Figure 51 shows the results of the transfer for the iPAQs to the i5150. As before, the data rate of the 192.168.0.15 is shown as the black line, while the red line is the data rate for 192.168.0.10. The blue line on the graph represents the sum of the individual data rates.

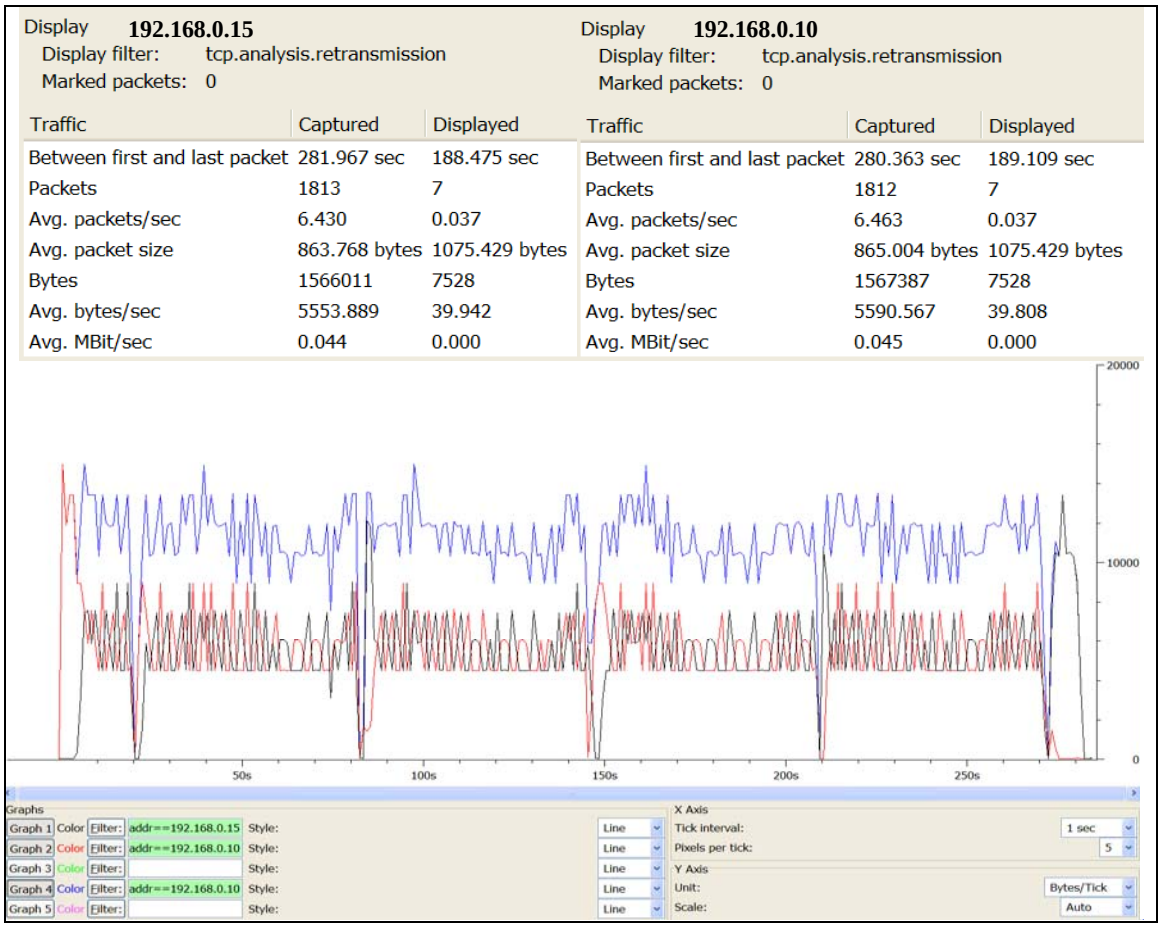

Figure 51. Both iPAQs transmit to i5150, and 192.168.0.15 acts as a relay

Figure 52 provides the summary of the entire transfer to the i5150.

Display **192.168.0.15 and 192.168.0.10**
Display filter: tcp.analysis.retransmission
Marked packets: 0

Traffic	Captured	Displayed
Between first and last packet	285.651 sec	251.711 sec
Packets	3625	14
Avg. packets/sec	12.690	0.056
Avg. packet size	864.386 bytes	1075.429 bytes
Bytes	3133398	15056
Avg. bytes/sec	10969.342	59.815
Avg. MBit/sec	0.088	0.000

Figure 52. Total summary of both iPAQs transmitting to the i5150, while 192.168.0.15 acts as a relay

The results shown in Figures 51 and 52 are very similar to the previous results in Figures 45 and 46 when the iPAQs communicated directly to the i9300 and did not use a relay. This is another indication that the additional hop at high data rate does not produce large amounts of delay or packet errors, even when the iPAQs are sharing the link to communicate.

Finally, the iPAQs both transmitted to the i9300 using the previous relay configuration. Figure 53 shows the results for the individual iPAQs with the blue line on the graph indicating the combined data rate for the link.

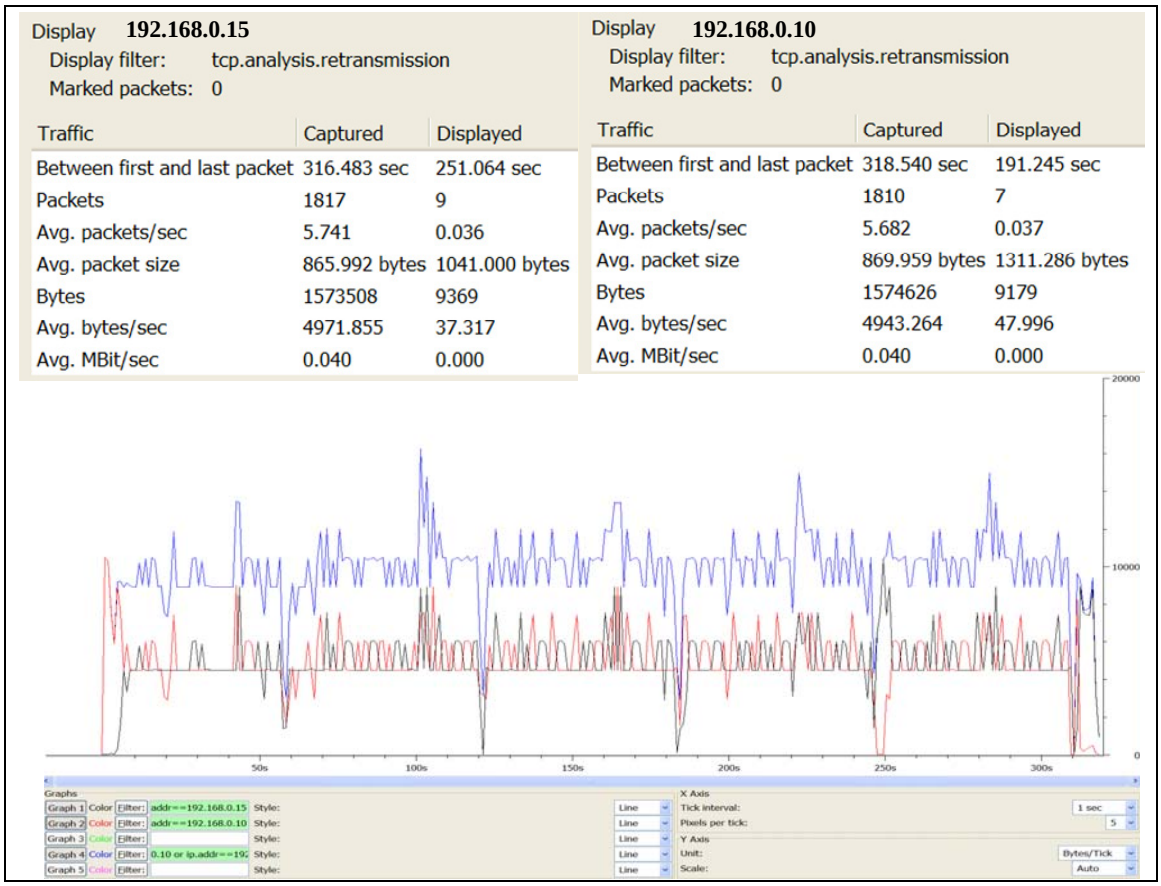

Figure 53. Both iPAQs transmit to i9300, and 192.168.0.15 acts as a relay

Figure 54 provides the overall results for the iPAQs' transmission to the i9300 using 192.168.0.15 as a relay. Again, this Wi-Fi only network does not have a higher average data rate or significantly less packet retransmissions.

Display **192.168.0.15 and 192.168.0.10**
Display filter: tcp.analysis.retransmission
Marked packets: 0

Traffic	Captured	Displayed
Between first and last packet	319.502 sec	251.064 sec
Packets	3627	16
Avg. packets/sec	11.352	0.064
Avg. packet size	867.972 bytes	1159.250 bytes
Bytes	3148134	18548
Avg. bytes/sec	9853.254	73.877
Avg. MBit/sec	0.079	0.001

Figure 54. Total summary of both iPAQs transmitting to the i9300, while 192.168.0.15 acts as a relay

D. CHAPTER SUMMARY

Analysis was performed on data transfers across a computer network that used RF links and a FSO link. Two iPAQ Pocket PC's sent a file across this network to a laptop in a variety of configurations, and the resulting data rate and the number of TCP retransmissions were recorded. When the iPAQs sent data files simultaneously, the time to transfer the files took roughly twice as long as when they transmitted only one file. It was shown that the end to end data rate was not limited by the FSO portion of the link and that additional hops at high data rate had no significant impact in the overall data rate or number of packets containing errors. The ship-UAV-satellite architecture should perform at least as well in terms of error rate and data throughput. The ship to ship antennas could be directional as opposed to the omnidirectional antennas used on the iPAQs and the RF links could operate simultaneously without interference by using different frequencies.

The next chapter discusses the conclusions of this research and presents recommendations for future work.

THIS PAGE INTENTIONALLY LEFT BLANK

VII. CONCLUSION AND FUTURE WORK

A. CONCLUSION

This thesis examined the required components and parameters necessary for a communications system that includes an RF link from a ship to a UAV and a FSO link from the UAV to a satellite. A brief discussion was made of the Transformational Communications Architecture in development and the network-centric operations it can enable. It was shown that by using an FSO-enabled UAV as a relay, a substantial improvement in data rate could be made and the size of the user's antenna can be reduced from a current satellite communication system. The WSC-6 (V) 9 has a 1.52 m antenna and communicates at a 2.048 Mbps capacity with the DSCS III satellite. The ship-UAV-satellite system communicates at 2 Gbps with a 1 ft antenna. A survey of possible UAV candidates and their potential to function as a high-altitude node was conducted. An experiment was done showing that the additional routing of information and the inclusion of an FSO link did not negatively affect the overall data transfer.

Since a high altitude UAV is more than three orders of magnitude closer to the earth's surface than a geostationary satellite, the link budget margin for a ship to UAV link greatly increases compared to a link from ship to satellite. This surplus margin can be used to increase the data rate and reduce the size of the antenna. The high bandwidth and large data rate capacity of FSO links cannot be realized in heavy fog, therefore fitting the FSO transceiver to a UAV in the upper atmosphere helps to ensure continuous operational capability. Several HALE UAVs currently in operation or in development are suitable for use as an airborne router. Experimental results from chapter VI indicate that in configurations where the supported data rate of the RF link is slower than the FSO link, the additional routing and optical transmission do not cause an increase in packet errors or a decrease in data rate.

B. FUTURE WORK

This thesis focused on the feasibility of a ship-UAV-satellite communications architecture on the link level. The expansion of the individual link to a network, or a

network of networks is needed to show how it can perform in FORCEnet or the TCA. When multiple units are within range of the UAV, the throughput of the composite link should be analyzed.

A software-based simulation and networking model with the ability to support different link characteristics could be developed. As shown in this thesis, different wavelengths of electromagnetic radiation are transmitted through the atmosphere with varying degree. Since the amount of received power and signal to noise ratio can affect BER, or data rate for a fixed BER, simulation of various transmission frequencies and several networking configurations in different environmental conditions could show widespread operational feasibility.

In order for the UAV to serve multiple ships in a strike group at the same time, aspects of the RF antenna and radio system should be explored. By sacrificing gain in a single direction, a low directivity antenna could be used to expand the field of view. Alternatively, a multi-beam phased array antenna could be installed. To prevent interference among users, a method to share the RF channel is required. Whether this is accomplished by frequency division multiple access, code division multiple access, or another scheme, removing traffic problems caused by multiple users is necessary to maximizing the benefit of the multiple ship-UAV-architecture.

LIST OF REFERENCES

[1] Little, Laura. "Enabling Network-Centric Operations. J6 Perspective." Presentation. http://www.oft.osd.mil/initiatives/ncw/presentations/nco_J6_perspective.cfm. Last accessed August 2005.

[2] Office of Force Transformation. "The Implementation of Network-Centric Warfare." Government Printing Office. January 2005.

[3] CJCSI 6250.01B. "Satellite Communication." Chairman of the Joint Chiefs of Staff Instruction. May 2004.

[4] Enabling Capabilities. "Transformational Communications Architecture." Marine Corps Concepts and Programs 2005. http://hqinet001.hqmc.usmc.mil/p&r/concepts/2005/toc1.htm. Last accessed August 2005.

[5] Regan, Mike. "TCA Brief to Defense News," presented 15 November 2004.

[6] Anderson, Christine. "Transformational Communications." March 2002. http://sunset.usc.edu/GSAW/gsaw2002/s8/canderson.pdf. Last accessed August 2005.

[7] FORCEnet. "What is FORCEnet." http://forcenet.navy.mil/What_Is/what_is_fn.htm. Last accessed August 2005.

[8] Mayo, Richard W, and Nathman, John. "ForceNet: Turning Information into Power." *USNI Proceedings*. February 2003.

[9] Proakis, John G. "Digital Communications." McGraw-Hill. 2001. 4th Edition.

[10] Eaglesfield, Charles C. "Laser Light. Fundamentals and Optical Communication." Macmillan and Company Limited. 1967.

[11] Wilson, Robert W. "The Cosmic Microwave Background Radiation." Nobel Lecture, 8. December 1978.

[12] Oliver, B. M. "Some Potentialities of Optical Masers." *Proceedings of the IRE*. Vol. 50. 1961.

[13] Einarsson, Göran. "Principles of Lightwave Communications." John Wiley and Sons, Inc. 1996.

[14] Sklar, Bernard. "Digital Communications. Fundamentals and Applications. 2nd ed." Prentice-Hall, Inc. 2001.

[15] Megla, Gerhard K. "Some New Aspects for Laser Communications." *Applied Optics.* Vol. 2, No. 3. March 1963.

[16] Gagliardi, Robert and Karp, Sherman. Optical Communications. John Wiley and Sons, Inc. 1976.

[17] Gagliardi, Robert M., and Karp, Sherman. "M-ary Poisson Detection and Optical Communications." *IEEE Trans. On Communication Technology*, 17-2, April 1969, 208-216.

[18] Roddy, Dennis. "Satellite Communications." McGraw-Hill. 3rd Edition. 2001.

[19] Klein, B. J., and Degnan, J. J. "Optical Antenna Gain. 1: Transmitting Antennas." *Applied Optics,* Vol. 13, No. 9. September 1974.

[20] Lambert, Stephen G., and Casey, William L. "Laser Communications in Space." Artech House Inc. 1995.

[21] Degnan, John J., and Klein, Bernard J. "Optical Antenna Gain. 2: Receiving Antennas," *Applied Optics,* Vol. 13, No. 9. 1974.

[22] Killinger, Dennis. "Free Space Optics. For Laser Communication Through the Air." *Optics and Photonics News*. October 2002.

[23] Petrin, R.R. et. al. **"**Atmospheric effects on CO_2 differential absorption lidar performance." Geoscience and Remote Sensing Symposium, 1996. IGARSS '96. 'Remote Sensing for a Sustainable Future,' International Volume 1. May 1996.

[24] Landis, G.A. **"**Space Power by Ground-Based Laser Illumination." *Aerospace and Electronic Systems Magazine*, IEEE Volume 6, Issue 11, Nov. 1991.

[25] Ha, Tri. "Digital Satellite Communications." McGraw-Hill. 2nd Edition. 1990.

[26] Janes. "AN/WSC-6/6A(V)9 Navy Multiband Shipboard Terminal." Jane's Military Communications. http://www.janes.com/ Last accessed July 2005.

[27] DSCS Certification Readiness Test Report. Harris Corporation. Document No. 7007960.

[28] Jane's. "DSCS III Series." Jane's Military Satellites – Communications. March 2004. http://www.janes.com Last accessed July 2005.

[29] Wright, C. H. G.; Heckert, G. P.; Bleier, T. E. "Near Term Approach to Data Relay for Satellites Under Test." *IEEE Transactions on Aerospace and Electronic Systems*. Vol 30, No. 3. July 1994.

[30] Terabeam Elliptica 7421 High-Performance Transceiver. Specifications. http://www.photonics.org/app/forums/attachments/TerabeamElliptica7421.pdf Last accessed August 2005.

[31] Hughes, Harold K. "Beer's Law and the Optimum Transmittance in Absorption Measurements." *Applied Optics.* Vol 2, No 9. September 1963.

[32] PLEXUS Release 3.0 Version 2.0. June 2003. http://www.vs.afrl.af.mil/ProductLines/IR-Clutter/plexus.aspx Last accessed July 2005.

[33] Foschini, Gerard J. and Greenstein, Larry J. "Spectral Efficiency of Optical FDM Systems Impaired by Phase Noise." IEEE Transactions on Communications. Vol. 41, No. 1. January 1993.

[34] Roddy, Dennis. "Satellite Communications." McGraw-Hill. 3rd Edition. 2001.

[35] Terabeam Transceiver Installer. Installation Software for Terabeam Transceiver. Terabeam Corporation. 2004.

[36] Cisco 12008 Series Router. Data Sheet. http://www.cisco.com/warp/public/cc/pd/rt/12000/prodlit/gsr_ov.pdf. Last accessed September 2005.

[37] Sweetman, Bill. "Endurance Above all for UAVs." Jane's International Defence Review. June 2003.

[38] Jane's. "GA-ASI MQ-1 and RQ-1 Predator." Jane's Unmanned Aerial Vehicles and Targets. March 2005.

[39] Jane's. "GA-ASI MQ-9 Predator B, Altair and Mariner." Jane's Unmanned Aerial Vehicles and Targets. March 2005

[40] Jane's. "Northrop Grumman RQ-4 Global Hawk." Jane's Unmanned Aerial Vehicles and Targets. March 2005.

[41] Jane's. "AeroVironment Centurion/Helios." Jane's Unmanned Aerial Vehicles and Targets. March 2004.

[42] Jane's. "Frontier Systems A160 Hummingbird." Jane's Unmanned Aerial Vehicles and Targets. March 2004.

[43] U.S. Navy Fact file. "SH-60 Seahawk Helicopter." http://www.navy.mil/navydata/fact_display.asp?cid=1200&tid=500&ct=1. Last accessed August 2005.

[44] Jane's. "Lockheed Martin 420K." Jane's Unmanned Aerial Vehicles and Targets. January 2005.

[45] "Technology for High Altitude Platforms." http://www.techspheresystems.com/DesktopDefault.aspx?TabId=6. Last accessed August 2005.

[46] Techsphere. "Wireless Communications." http://www.techspheresystems.com/DesktopDefault.aspx?TabId=24. Last accessed August 2005.

[47] Minor, Elliot. "Georgia Company to Demonstrate a Defense Airship Near Washington." Associated Press. June 2004.

[48] Business Wire. "Sierra and Techsphere Recieve Order for High Altitude Airship." January 2005.

[49] Stallings, William. "High-Speed Networks and Internets." Prentice Hall. 2nd ed. 2002.

[50] Monterey, California Hourly Observations by Intellicast. http://www.intellicast.com/Local/USLocalStd.asp?loc=kmry&seg=LocalWeather&prodgrp=CurrentWeather&product=HourlyObservations&prodnav=none. Last accessed August 2005.

[51] Stallings, William. "Wireless Communications and Networks." Pearson Prentice Hall. 2nd ed. 2005.

[52] Sharpe, Richard. "Just what is SMB?" http://samba.anu.edu.au/cifs/docs/what-is-smb.html. Last Accessed August 2005.

[53] Trident Warrior 2003. Video clip. https://tlnst.spawar.navy.mil/. Last accessed August 2005.

[54] Crawford, Sharon. "Building Bridges." Windows XP Home Networking. http://www.microsoft.com/windowsxp/using/networking/expert/crawford_02april22.mspx. Last accessed September 2005.

INITIAL DISTRIBUTION LIST

1. Defense Technical Information Center
   Ft. Belvoir, VA

2. Dudley Knox Library
   Naval Postgraduate School
   Monterey, CA

3. Ms. Michelle Bailey
   SPAWAR Systems Center
   San Diego, CA

4. Mr. Donald Endicott
   SPAWAR Systems Center
   San Diego, CA

5. Mr. Fernando Escobar
   SPAWAR Systems Center
   San Diego, CA

6. Mr. W. Dale Bryan
   SPAWAR Systems Center
   San Diego, CA

7. Dr. Michael Lovern
   SPAWAR Systems Center
   San Diego, CA

8. Dr. Roy Axford
   SPAWAR Systems Center
   San Diego, CA

9. Dr. Karl Moeller
   SPAWAR Systems Center
   San Diego, CA

10. Dr. Rich North
    SPAWAR Systems Center
    San Diego, CA

11. RADM Victor See
    Pentagon
    Arlington, VA

12. Mr. Michael Regan
SPAWAR-SFA
Chantilly, VA

13. Mr. David Gilliam
National Reconnaissance Office
Chantilly, VA

14. CAPT Luke Lukenbill
National Reconnaissance Office
Chantilly, VA

15. Lt. Col. Michael Ward
National Reconnaissance Office
Chantilly, VA

16. Dr. Peter Goetz
Naval Research Lab
Washington, D.C.

17. Dr. Frank Kragh
Naval Postgraduate School
Monterey, CA

18. Dr. Tri Ha
Naval Postgraduate School
Monterey, CA

19. Dr. R. Clark Robertson
Naval Postgraduate School
Monterey, CA

20. Dr. David Netzer
Naval Postgraduate School
Monterey, CA

21. Dr. Donald Walters
Naval Postgraduate School
Monterey, CA

22. Chair, Electrical and Computer Engineering Department
Naval Postgraduate School
Monterey, CA

23. Ms. Rita Painter
Naval Postgraduate School
Monterey, CA

24. LT Kenneth St. Germain
USS SHOUP (DDG-86)
FPO-AP 96678-1300